

General suggestions:

If a two-part option is adopted for publishing this dataset, I feel that the manuscript can be further improved to make it clearer of this intention, the purpose and the focus of part I and the main topics to be included in part II. Some parts of text need to be revised - some new to be added and some existing ones moved to part II.

The part I paper focuses on the long-term measurement activities at WLG, use of different statistical methods to derive trends, and reporting the overall diurnal/seasonal/long-term variations, especially the intriguing findings of larger rates of increase in ozone in autumn and spring. You can add more on quality assurance activities for the long-term data collection and elaborate on use of different statistical methods to derive the trends. Some general/vague discussions on underlying factors/processes can be omitted from part I but strengthened in part II.

Specific suggestions:

- 1. Abstract: state the purpose of this part I paper so that the reader will be clear of your plan of presenting the data. Make the abstract more concise. Line 14-15 “the levels of ...meteorological conditions” can be omitted. Rephrase the last sentence of the abstract.***

We thank the editor for this suggestion and have made according changes to the abstract. Please refer to the marked-up version of the revised manuscript for details.

- 2. Introduction: This part may need major re-write. If you plan to include detail dynamic/chemical processes in part II, then the detailed reviews of these processes are not needed here, because you would include them the introduction of part II.***

We thank the editor for the valuable suggestion, which we fully agree with. The detail on the influencing factors of surface ozone were deleted from this work and will be added to the part II paper. In addition, we have included a new paragraph reviewing methods that were used in literatures to analyze ozone trends and variability. The advantage of the methods we used are highlighted. The aim of this work (part I) and that of the part II study is briefly stated at the end of the

introduction, to let the reader know what information this work provides and what can be found in the next one.

3. *Page 3, line 13 “Long-term trends in ozone in China, ...”. Do you refer long-term to >20 years? Several studies of the medium term (10-15 years) ozone are listed in the reviews afterwards.*

Response: “long-term” here was referring to the studies that were listed afterwards. Although 10-15 years would be considered medium term in a climatological sense, atmospheric ozone measurements of such a timescale in China are very scarce and have already been considered as long-term measurements in these works. To make that clear, this part was rephrased in the revised manuscript.

4. *Line 25-28, consider rephrasing the statement. These previous studies in polluted parts of China have different purpose from that at WLJ. They reflect mainly impact of emissions in polluted eastern China, whereas WLJ looks into background troposphere in remote continental Asia and long-range transport impact.*

Response: This part was rephrased into:

“The above studies all focus on the most polluted regions in the eastern part of China, i.e., the NCP, YRD and PRD, aiming to study the impact of growing precursor emissions on ozone trends. The trend of ozone over remote background regions in China still remains to be studied based on long-term observations.”

5. *Page 4, line 1-3: consider rephrasing the sentence. Line 24-31: comments on the previous studies are not quite accurate. These previous studies aimed at short-term processes influencing diurnal, episodic, and seasonal variations. They are not for more-term trend. The present study has its clear new advancement compared the short-time studies, no need to ‘criticize’ these short-term studies for their different focus.*

We certainly did not intend to “criticize” any of these studies. We only wanted to

point out that we are still in lack of long-term trend studies at Waliguan. To make that clear we rephrased this part into: “Previous studies of ozone at WLG, based on short-term measurements and modelling results, clarified the causes for certain episodes or for the diurnal and seasonal cycle of ozone (Ma et al., 2002a;Ma et al., 2005;Zhu et al., 2004). The overall variation characteristics and long-term trend of ozone at WLG have not yet been studied.”

6. ***The results and discussion part: refer to general comments. The factors influencing diurnal variation, events, and summer peak have been examined in previous studies; the discussions of the present paper can focus more on overall trend and year-to-year variations.***

We agree with the editor and have accordingly made some changes, please refer to the marked-up revised manuscript for details.

7. ***Summary: make it more concise. Line 22-25 on the cause of diurnal variation and summer peak can be removed as these have been known in previous studies.***

We have made the summary part more concise by deleting the cause of the diurnal variation and summer peak and some vague conclusions as suggested.

Long-term trends of surface ozone and its influencing factors at the Mt. Waliguan GAW station, China, Part 1: Overall trends and characteristics.

W. Y. Xu¹, W. L. Lin², X. B. Xu^{1,*}, J. Tang², J.Q. Huang³, H. Wu³, X.C.Zhang²

[1] State Key Laboratory of Severe Weather & Key Laboratory for Atmospheric Chemistry, Institute of Atmospheric Composition of China Meteorology Administration, Chinese Academy of Meteorological Sciences, Beijing, China

[2] Meteorological Observation Center, China Meteorological Administration, Beijing, China

[3] Waliguan Observatory, Qinghai Meteorological Bureau, Xining, China

* Correspondence to: X. B. Xu (xuxb@cams.cma.gov.cn)

Abstract

~~Tropospheric ozone is an important atmospheric oxidant, greenhouse gas and atmospheric pollutant at the same time. The level of tropospheric ozone, particularly in the surface layer, is impacted by emissions of precursors and is subjected to meteorological conditions. Due its importance, the long~~Long-term variation trend of baseline ozone is highly needed information for environmental and climate change assessment. So far, studies about the long-term trends of ozone at representative sites are mainly available for European and North American sites. Similar studies are lacking for China, ~~a country with rapid economic growth for recent decades,~~ and many other developing countries. ~~To uncover the long-term characteristics and trends~~Measurements of baseline surface ozone, mixing ratio in western China, measurements were carried out at a global baseline Global Atmospheric Watch (GAW) station in the north-eastern Tibetan Plateau region (Mt. Waliguan, 36°17' N, 100°54' E, 3816m a.s.l.) for the period of 1994 to 2013 ~~were analysed in this study. Results reveal higher surface ozone during the night and lower during the day at Waliguan caused by mountain valley breezes and a seasonal maximum in summer.~~ To uncover the variation characteristics, long-term trends and influencing factors of surface ozone at this remote site in western China, a two-part study has been carried out, with this part focusing on the overall characteristics of diurnal, seasonal and

带格式的

1 long-term variations and the variation trends of surface ozone. To obtain reliable ozone trends,
2 we performed the Mann-Kendall trend test and the Hilbert-Huang Transform (HHT) analysis
3 on the ozone data. Our results confirm that the mountain-valley breeze plays an important role
4 in the diurnal cycle of surface ozone at Waliguan, resulting in higher ozone values during the
5 night and lower ones during the day, as was previously reported. Systematic diurnal and
6 seasonal variations were found in mountain-valley breezes at the site, which were used in
7 defining season-dependent daytime and nighttime periods for trend calculations. Significant
8 positive trends in surface ozone were detected for both daytime (2.4 ± 1.6 ppbv $10a^{-1}$) and
9 nighttime (2.8 ± 1.7 ppbv $10a^{-1}$). ~~Nighttime ozone mixing ratios are more representative of the~~
10 ~~free tropospheric condition, with~~The largest nighttime increasing rate occurred in autumn
11 (2.9 ± 1.1 ppbv $10a^{-1}$) ~~and), followed by~~ spring (2.4 ± 1.2 ppbv $10a^{-1}$) ~~revealing the largest~~
12 ~~increase rates, while),~~ summer (2.2 ± 2.0 ppbv $10a^{-1}$) and winter (1.3 ± 1.0 ppbv $10a^{-1}$) ~~show~~
13 ~~weaker increases. Spectral), respectively. The HHT spectral~~ analysis identified four different
14 episodes with different positive trends, with the largest increase occurring around May 2000
15 and Oct. 2010. ~~A~~The HHT results suggest that there were ~~2-4 year, 7 year~~4a, 7a and 11 year
16 ~~periodicity was found~~11a periodicities in the timeseries of surface ozone mixing ratio at
17 Waliguan. The results ~~are highly valuable for~~of this study can be used in related climate and
18 environment change assessments ~~of western China and surrounding areas, and for~~and in the
19 validation of chemical-climate models.

带格式的

21 **1 Introduction**

22 Ozone (O_3) is one of the key atmospheric species and is closely related to climate change and
23 environmental issues (IPCC, 2013). The stratospheric ozone layer protects living organisms at
24 the Earth's surface against the harmful solar UV radiation, while tropospheric ozone is an
25 important greenhouse gas and governs oxidation processes in the Earth's atmosphere through
26 formation of OH radical (Staelin et al., 2001; Lelieveld and Dentener, 2000). In the surface
27 layer, ozone is also one of the toxic gases for human beings and vegetation.

28 ~~Since stratospheric ozone is much higher in mixing ratio than tropospheric ozone, it can be well~~
29 ~~monitored by satellites with retrieved column density. However, ozone in~~Data about the
30 ~~troposphere, particularly surface~~spatiotemporal variations of ozone ~~is~~have been highly variable
31 ~~in space~~needed for assessing the impacts of ozone on human health, ecosystem, and
32 ~~time.~~climate. Since ozone is a secondary gas pollutant, ~~observed surface concentrations are~~its

1 mixing ratio is influenced both by local photochemistry and by transport ~~processes~~ of ozone
2 ~~or~~ and its precursors (Wang et al., 2006a; Lal et al., 2014) ~~from nearby locations~~. Deep
3 convection and stratosphere-to-troposphere exchange (STE) events can also bring down ozone-
4 rich air from above and influence surface ozone mixing ratios at high-elevation sites (Bonasoni
5 et al., 2000; Ding and Wang, 2006; Stohl et al., 2000; Tang et al., 2011; Lefohn et al., 2012; Jia et
6 al., 2015; Ma et al., 2014; Langford et al., 2009; Langford et al., 2015; Lin et al., 2012a; Lin et al.,
7 2015a). ~~All these influencing factors make it very hard to obtain the background ozone mixing~~
8 ~~ratio and to understand the causes of observed ozone trends.~~ In the troposphere, particularly in
9 the surface layer, ozone is highly variable in space and time due to the large variabilities of its
10 dominant sources and sinks, which are impacted by anthropogenic activities and meteorological
11 conditions. So far, there has been no better way than networked monitoring to obtain the spatial
12 distribution and temporal variation of ozone.

13 ~~Many~~ The Global Atmosphere Watch (GAW) ~~stations~~ programme of the World Meteorological
14 Organization (WMO) ~~and environmental~~ has been one of the key international initiatives in
15 long-term monitoring ~~sites of the chemical and physical properties of the atmosphere.~~ Many
16 GAW stations have been ~~setup~~ set up to monitor air compositions including surface ozone due
17 to its importance and due to the urgent need to evaluate the trends of background ozone.
18 ~~Past~~ Based on data from some GAW sites and other sources, past trends in surface background
19 ozone have been reported for Europe and North America (Cooper et al., 2010; Cui et al.,
20 2011; Gilge et al., 2010; Oltmans et al., 2013; Vingarzan, 2004; Parrish et al., 2012; Logan et al.,
21 2012), which mostly revealed strong increases in ozone before 2000 and slow or even no growth
22 afterwards. Data from some important regions, e.g., East Asia and South America, are very
23 scarce, which make them even more valuable. China, as one of the rapidly developing countries,
24 is contributing increasing ozone precursor ~~mixing ratio~~ emissions to the atmosphere and was
25 thought to be most responsible for the increase in ozone in the western United States (Cooper
26 et al., 2010), though other studies ~~would~~ suggest that STE events had an equivalent important
27 role in causing high-ozone events at western U.S. alpine sites during spring (e.g. Langford et
28 al., 2009; Ambrose et al., 2011; Lin et al., 2012a; Lin et al., 2015a). A recent study by Lin et
29 al. (2015b) found that although rising Asian emissions contribute to increasing springtime
30 baseline ozone over the western U.S. from the 1980s to the 2000s, the observed western US
31 ozone trend over the short period of 1995-2008 previously reported by Cooper et al. (2010) has
32 been was strongly biased by meteorological variability and measurement sampling artefacts.

1 Nevertheless, the impact of Asian pollution outflow events on western US surface ozone is
2 evident (Lin et al., 2012b; Lin et al., 2015a).

3 Besides the impact of Asian pollution outflow on the surface ozone in other regions, it is at least
4 equally important to know how the level of surface ozone in Asia, particular in China, has been
5 changing. Long-term ~~trends~~ changes in ozone in China, however, ~~were seldom~~ have only been
6 reported: in a few publications. Ding et al. (2008) studied the tropospheric ozone climatology
7 over Beijing based on ~~aircraft data~~ data from the MOZAIC (Measurement of Ozone and Water
8 Vapor by Airbus In-Service Aircraft) program and found a 2% yr⁻¹ increase of boundary layer
9 ozone from the period of 1995-1999 to 2000-2005 ~~in~~ over Beijing in the North China Plain
10 (NCP) region, ~~which was mostly driven by the increasing anthropogenic emissions in the~~
11 ~~surrounding regions. Upper tropospheric ozone displayed~~ and a weaker increasing trends. ~~trend~~
12 of free-tropospheric ozone. Wang et al. (2012) reported a similar increasing trend of lower
13 tropospheric ozone and ~~a larger~~ ozone increases in the middle and upper tropospheric ozone
14 ~~increase~~ troposphere for the period of 2002 ~~to~~ 2010 based on ozone sonde measurements ~~in~~ over
15 Beijing. Xu et al. (2008) ~~observed~~ reported positive trends of extreme values and increased
16 variability in ~~ozone~~ 6 periods of ozone measurements from 1991 to 2006 at Lin'an, a
17 background site in the Yangtze River Delta (YRD) region. Wang et al. (2009) found a
18 significant increasing trend of 0.58 ppbv yr⁻¹ during 1994 ~~to~~ 2007 at a coastal site of Hong
19 Kong in the Pearl River Delta (PRD) region, which ~~were~~ was caused by rapid increases in ozone
20 precursor emissions in the upwind source regions. The above studies ~~were~~ all carried out focus
21 on the most polluted regions in the eastern part of China, ~~in i.e., the three most polluted regions~~
22 NCP, YRD and PRD, ~~where observed ozone mixing ratios were mainly under the influence of~~
23 ~~regional air pollution and are not representative of the~~ aiming to study the impact of growing
24 precursor emissions on ozone trends. The trend of ozone over remote background ~~ozone level~~
25 on a larger scale. The trends of ozone over other parts of China remain regions in China still
26 remains to be studied based on long-term observations.

27 Continuous long-term observations of surface ozone ~~are~~ have been made only at a few
28 representative sites in China, among which is the Mt. Waliguan (WLG) GAW station, one of
29 the high altitude stations of the GAW network. The WLG station, established in 1994, has the
30 longest ozone measurement record in China and is situated ~~in~~ at the northeastern edge of the
31 Tibetan Plateau, where population is scarce and industries hardly exist. It is a pristine high
32 elevation site located downwind of the European, Central Asian and Indian outflow,

1 representative of the background of the Eurasian continent. A few studies have already been
2 performed on short-term measurements of ozone at WLG. ~~Past research already revealed that~~
3 ~~surface~~Surface ozone at the site ~~is~~has been proved to be highly representative of free-
4 tropospheric ozone (Ma et al., 2002b) and ~~hence is often influenced by stratosphere-subjected~~
5 ~~to-troposphere-exchange-(the influences of STE)~~ events (Ding and Wang, 2006;Zhu et al.,
6 2004). Air masses from the west are dominant at WLG and were found to be associated with
7 the highest ozone mixing ratios (Wang et al., 2006b). Only in summer a substantial part of the
8 airflows come from the eastern sector and exposes the surface ozone mixing ratio to some
9 regional anthropogenic influences (Wang et al., 2006b;Xue et al., 2011). Previous studies of
10 ozone at WLG, based on short-term measurements and modelling results, clarified the causes
11 for certain episodes or for the diurnal and seasonal cycle of ozone (Ma et al., 2002a;Ma et al.,
12 2005;Zhu et al., 2004). ~~Other than STE, meteorological factors with very short timescales such~~
13 ~~as the diurnal cycle in topographic wind or with very long timescales such as the solar cycle~~
14 ~~also have significant impacts on tropospheric ozone at WLG . QBO (Quasi-Bi-annual~~
15 ~~Oscillation) and ENSO (El Niño and Southern Oscillation) have been shown to influence total~~
16 ~~ozone burdens over the Tibet . This influence could extend to the lower troposphere via STE~~
17 ~~and thus affect ozone variability measured at the 3.8 km altitude of WLG. A few studies~~
18 ~~suggested that the change in dynamics after El Niño events can promote the cross-tropopause~~
19 ~~ozone-exchange and lead to a rise in global mean tropospheric ozone concentration . Over western~~
20 ~~U.S. high elevation regions prone to deep stratospheric intrusions, however, found that the~~
21 ~~increased frequency of deep tropopause folds that form in upper-level frontal zones following~~
22 ~~strong La Niña winters exerts a stronger influence on springtime ozone levels at the surface~~
23 ~~than the El Niño-related increase in lower stratospheric ozone burden. The Tibetan Plateau has~~
24 ~~also been identified as a preferred region for deep stratospheric intrusions . The extent to which~~
25 ~~ENSO events, jet characteristics and STE modulate inter-annual variability of lower~~
26 ~~tropospheric ozone at WLG requires further investigation. The overall variation characteristics~~
27 ~~and long-term trend of ozone at WLG have not yet been studied. Considering the geographical~~
28 ~~representativeness of the WLG site, results on the long-term variations of ozone at WLG may~~
29 ~~add more understanding of ozone changes in the northern mid-latitudes, particularly the~~
30 ~~hinterland of the Eurasian continent.~~

31 The most common method used in the detection of ozone trends is the linear least squares
32 method (Tarasova et al., 2009;Cui et al., 2011;Wang et al., 2009;Xu et al., 2008). Other studies
33 directly compared mean ozone levels of different periods to detect possible trends (Ding et al.,

1 2008;Lin et al., 2014). Oltmans et al. (2013) used the Theil-Sen estimate together with the
2 Mann-Kendall's tau test to determine trends and their significance in the W126 and W_{Low}
3 metrics. The non-linear variation of ozone mixing ratio with season and many other climatic
4 factors can introduce uncertainties into the linear trend analysis. Wang et al. (2012)
5 deseasonalized the monthly data by subtracting the average of all monthly data for a given
6 month from the original data of the same month before performing a linear regression analysis.
7 (Oltmans et al., 2006;Oltmans et al., 2013) first performed an autoregressive model fitting
8 incorporating explanatory variables (that are known sources of ozone variability) and a cubic
9 polynomial fit to better represent the long-term variations of ozone, then used a bootstrap
10 method to determine the trends of ozone. However, surface ozone typically is influenced by
11 many factors, which makes it hard to determine which to incorporate. The seasonal Mann-
12 Kendall test, which is a modified version of the non-parametric Mann-Kendall trend test, can
13 account for the seasonal variation within the data Hamed and Ramachandra Rao (1998). It has
14 been widely applied in hydrology and seldom in atmospheric chemistry. The Hilbert-Huang
15 Transform (HHT) analysis, which has been widely applied on the analysis of meteorological
16 datasets and not yet on that of atmospheric composition data, is a precise and adaptive spectral
17 analysis method, that can divide the signal into various oscillation modes and study the anomaly
18 and periodicity within the data (Rao and Hsu, 2008). Applications of HHT on temperature,
19 wind, rainfall and solar radiation data have proved that the HHT method is capable of capturing
20 synoptic and climatic features, revealing known diurnal, seasonal, annual and inter-annual
21 cycles (Huang, 2014)~~Previous studies of ozone at WLG were all based on short-term~~
22 ~~measurements and were mostly model-based mechanism studies on the causes of the ozone~~
23 ~~seasonal cycle, which did not lead to consensus and brought upon debates , while the overall~~
24 ~~variation characteristics and long-term trend of ozone at WLG remain unclear. In this study, we~~
25 ~~present an analysis of 20-year surface ozone mixing ratio at WLG. Besides unravelling the~~
26 ~~characteristics of ozone variations and the overall variation trend of ozone, a precise and~~
27 ~~adaptive spectral analysis method will be applied to investigate the trend during different~~
28 ~~periods and the underlying periodicities within the data.~~

29 .
30 In this paper, we present the first part of an analysis on 20-year surface ozone mixing ratio at
31 WLG, focusing mainly on the overall diurnal, seasonal and long-term variations characteristics
32 and the variation trends of surface ozone. We will apply a linear regression as well as a seasonal

Mann-Kendall test together with the Theil-Sen estimate to calculate the overall variation trend of ozone. The HHT spectral analysis method will be used for the first time to investigate the ozone trends during different periods and the underlying anomalies and periodicities within the ozone data. A detailed discussion on the influencing factors contributing to the ozone variation at WLG will be presented in a companion paper.

2 Data and Methodology

2.1 Site and Measurements

The Mt. Waliguan site (WLG, 36°17' N, 100°54' E, 3816 m asl) is located in Qinghai Province, China. It is one of the global baseline stations of the WMO/GAW network and the only one in the hinterland of ~~Eurasia~~the Eurasian continent. WLG is situated at the northeast edge of the Qinghai-Tibetan Plateau and surrounded by highland steppes, tundra, desserts, salt lakes, etc. (Figure 1). With very few population (about 6 persons km⁻²) and ~~nearly no~~hardly any industry within 30 km, the WLG site is far from major anthropogenic sources. However, some impact of long-range transport of anthropogenic pollutants from the NE-SE sector cannot be excluded, particularly from the major cities Xining (about 90 km northeast of WLG, population ~2.13 millions) and Lanzhou (about 260 km east of WLG, population ~3.1 millions). Such impact, if any, may be significant only during the warmer period (May-September), as suggested by ~~past~~previous air mass trajectory studies (Zhang et al., 2011).

The WLG baseline station was established in 1994. ~~Long~~The long-term monitoring program for surface ozone began in August 1994. The mixing ratio of surface ozone has been measured using two ozone analysers (Model 49, Thermal Environmental Instruments; one of the ~~analyzers~~analysers was replaced with a Model 49i ozone ~~analyzer~~analyser in 2011) at a sampling height of 7 meters. The analysers have been automatically zeroed alternatively every second day by introducing ozone-free air for 45 min. Seasonal multipoint calibrations (8 points) have been done using an ozone calibrator (Model 49PS, Thermal Environmental Instruments). The analysers have been checked weekly for changes in instrument parameters. The inlet filters have been replaced weekly. Maintenance on the observation system has been performed yearly and whenever it was necessary. The yearly maintenance includes cleaning of absorption tubes, pumps, inlet tubing and other connecting parts, and checking of the inlet loss. In the years 1994, 1995, 2000, 2004, and 2009, the ozone calibrator and analysers at WLG were compared with

1 the transfer standard from the WMO World Calibration Centre for Surface Ozone and Carbon
2 Monoxide, EMPA Dübendorf, Switzerland. Intercomparison results show excellent or good
3 agreement between the WLG instruments and the transfer standard (Zellweger et al.,
4 2000; Zellweger et al., 2004; Zellweger et al., 2009). Surface The two instruments performed
5 parallel measurements, recording surface ozone data ~~are recorded~~ as 5-minute averages ~~and,~~
6 which were corrected annually based on the zero-checks and multipoint calibrations. If the
7 observed ozone values from the two analysers ~~agree~~ agreed within 3 ppb, average values
8 ~~are were~~ calculated and included in the final dataset. Otherwise, causes for the differences
9 ~~are were~~ searched by the principal investigator and only data from the well-performing analyser
10 ~~are were~~ included in the dataset. 5-min 95% of the data pairs show discrepancies within ± 1.0 ppb
11 and the difference between two instruments shows a nearly random distribution around zero. 5-
12 minute averaged ozone mixing ratios from Aug. 1994 to Dec. 2013 were then averaged into
13 hourly data and used in this study. In the trend analysis, monthly average ozone mixing ratios
14 were acquired by first calculating the daily average ozone values and then performing a monthly
15 averaging. A data completeness of 75% was required for each averaging step.

16 Meteorological observations have been made at the site using automatic weather stations (AWS)
17 installed on the ground level and on an 80 m tower at 2, 10, 20, 40 and 80 m height. These
18 observations provide meteorological parameters such as temperature, pressure, precipitation,
19 and wind speed/direction in 5 min resolution. Additionally, the vertical velocity is measured at
20 the 80 m platform. The 10 m horizontal wind and 80 m vertical wind data from Aug. 1994 to
21 Dec. 2013 are used in this study and have been accordingly averaged into hourly data, which
22 meet a data completeness requirement of 75%.

23

24 **2.2 Determination of daytime and nighttime**

25 Past research has already revealed that the surface ozone at WLG is governed by different air
26 masses during daytime and nighttime (Ma et al., 2002b). The WLG station experiences upslope
27 winds during the day and is controlled by boundary layer (BL) air, while during the night, winds
28 go downslope and the site is controlled by free tropospheric (FT) air. The boundary layer air is
29 largely influenced by local photochemistry and ~~contains~~ may contain pollutants transported
30 from nearby areas, while the free-tropospheric air represents the background ozone and may
31 sometimes contain signals of long-range transport or STE events. Hence, it is of necessity to

1 differentiate between daytime and nighttime ozone mixing ratio in order to study the trend
2 signals brought by different air masses.

3 In the previous study (Xu et al., 2011)(~~Xu et al., 2011~~), daytime and the nighttime were defined
4 as ~~a~~ fixed time ranges (e.g. 11:00-16:00 LT for daytime and 23:00-4:00 LT for nighttime).
5 However, the actual well-developed day and night time ~~range varies~~ranges vary with season.
6 ~~So, and so~~ does the local wind. Figures 2a-c respectively show the season-diurnal variation
7 characteristics of 10 m zonal (u) and meridional (v) wind velocity and the 80 m vertical (w)
8 wind velocity. Due to the local topography, the WLG station is under the influence of mountain-
9 valley breezes and all three wind vectors exhibit distinct diurnal variation characteristics. The
10 height difference to the west of Mt. WLG is much larger than that to the east, hence valley
11 breezes during daytime come from the west accompanied by upward drafts, resulting in a
12 diurnal maximum u and w vector between noontime and middle afternoon depending on the
13 season. The v vector changes from southern ~~winds~~ to northern winds around noontime.
14 Mountain breezes during the night come from the east-south-east sector accompanied by
15 subsiding air flows, resulting in low u and w and high v during the night. The dominant air flow
16 at WLG is westerly during the cold seasons, which enhances the westerly valley breeze during
17 the day and cancels out the easterly mountain breeze during the night. During the warm seasons,
18 easterly winds gain in frequency, which sometimes cancels out the daytime valley breeze and
19 enhances the nighttime mountain breeze. The distinct diurnal variation of the wind can be used
20 to define a daytime and nighttime range that varies with season. The white dots in Figure 2
21 represent the monthly average occurrence hour of the diurnal maximum u . In this study, a 6
22 hour time range that is centred around the white dots is used as the daytime range (white dashed
23 lines in Figure 2). The nighttime window also covers 6 hours and is considered to be offset by
24 12 hours to the daytime window.

26 2.3 Trend analysis

27 The trend analysis was performed using ~~a~~ both the spearman's linear trend analysis and the
28 modified Mann-Kendall's trend test. The Mann-Kendall test is performed using a Fortran
29 program developed by Helsel et al. (2006). Here, a brief description on the modified Mann-
30 Kendall test will be given. The Mann-Kendall test is a non-parametric test commonly used to

1 detect trends. Hamed and Ramachandra Rao (1998) modified the test, so that it can be used on
2 data with seasonality.

3 For two sets of observations $X = x_1, x_2, \dots, x_n$ and $Y = y_1, y_2, \dots, y_n$, the rank correlation test as
4 proposed by (Kendall, 1955) is performed as the following:

$$5 \quad S = \sum_{i < j} a_{ij} b_{ij} \quad (1)$$

$$6 \quad \text{Where } a_{ij} = \text{sign}(x_j - x_i) = \begin{cases} 1 & x_i < x_j \\ 0 & x_i = x_j \\ -1 & x_i > x_j \end{cases} \text{ and } b_{ij} \text{ is the equivalent for } Y. \quad (2)$$

7 If Y is replaced with the time order $T = 1, 2, \dots, n$, the test becomes a trend test and $S = \sum_{i < j} a_{ij}$.

8 The significance of the trend is tested by comparing the standardized test statistic $Z =$
9 $S / \sqrt{\text{var}(S)}$ to the standard normal variate at a given significance level (Z_α). Here, a modified
10 $\text{var}(S)$ is given by:

$$11 \quad \text{var}(S) = \frac{n(n-1)(2n+5)}{18} \frac{n}{n_S^*}, \quad (3)$$

12 where $\frac{n}{n_S^*}$ represents a correction for the autocorrelation that exists in the data and can be
13 obtained by an approximation to the theoretical values.

$$14 \quad \frac{n}{n_S^*} = 1 + \frac{2}{n(n-1)(n-2)} \sum_{i=1}^n (n-i)(n-i-1)(n-i-2) \rho_s(i) \quad (4)$$

15 Here $\rho_s(i)$ is the autocorrelation function of the ranks of the observations.

16 If $|Z| > Z_{1-\alpha/2}$, then the data is non-stationary, a positive Z would indicate a positive trend and a
17 negative Z would suggest a declining trend. If $|Z| \leq Z_{1-\alpha/2}$, then the data is stationary. Here we
18 use $\alpha=0.05$, hence the corresponding critical $Z_{1-\alpha/2}=1.96$. A non-parametric method is then used
19 to estimate the slope of the trend, details can be found in Sen (1968).

20

21 **2.4 The Hilbert-Huang Transform analysis**

22 The Hilbert-Huang Transform (HHT) analysis is a combination of the Empirical Mode
23 Decomposition (EMD) and the Hilbert Spectral analysis proposed by Huang et al. (1998). It is
24 often used to analyse the time-frequency variation of non-linear and non-stationary processes.
25 The EMD acts as a time-frequency filter, it decomposes the data into several oscillation modes
26 with different characteristic time scales. The HHT method has been proved to be an efficient

1 and precise method in investigating the periodicity, long-term oscillations and trends that are
 2 embedded within the data (Huang and Wu, 2008). So far, it has been widely applied in
 3 atmospheric meteorological and climatic studies including wind field, temperature, radiation
 4 and rainfall analysis (Rao and Hsu, 2008; Lundquist, 2003; El-Askary et al., 2004), but it has not
 5 been used on atmospheric composition data yet. Here we give a brief description of the HHT
 6 method.

7 First, the EMD is performed on the data, to decompose the data into n intrinsic mode functions
 8 (IMF), c_1, c_2, \dots, c_n , and one residual r_n , which are ordered from the smallest to the largest
 9 variational variation time scale (Huang et al., 2003).

$$10 \quad x(t) = \sum_{j=1}^n c_j + r_n \quad (5)$$

11 Then the Hilbert transform is applied to each IMF using Eq. 6,

$$12 \quad y(t) = \frac{1}{\pi} P \int_{-\infty}^{\infty} \frac{x(t')}{t-t'} dt' \quad (6)$$

13 Where P is the Cauchy principal value. An analytical signal is then obtained with Eq.7,

$$14 \quad z(t) = x(t) + iy(t) = a(t)e^{i\theta(t)}, \quad (7)$$

$$15 \quad \text{where, } a(t) = [x^2(t) + y^2(t)]^{1/2} \text{ and } \theta(t) = \arctan\left(\frac{y(t)}{x(t)}\right). \quad (8)$$

16 The instantaneous frequency ω can be calculated as the following:

$$17 \quad \omega(t) = \frac{d\theta(t)}{dt}. \quad (9)$$

18 Thus, Eq.5 an can be transformed into the following expression:

$$19 \quad x(t) = \Re \sum_{j=1}^n a_j(t) \exp\left(i \int \omega_j(\tau) d\tau\right), \quad (10)$$

20 where \Re is the real part of the complex number.

21 To obtain the Hilbert amplitude spectrum spectrum $H(\omega, t)$, we assign for each time t , the
 22 calculated amplitude $a_j(t)$ to the according $\omega_j(t)$. An integration of $H(\omega, t)$ over the frequency
 23 span would yield yields the instantaneous energy (IE), which represents the time variation of
 24 the energy. An integration along the time span would yield yields the marginal Hilbert spectrum
 25 $h(\omega)$, which provides information on how the frequency is distributed over the entire span.

26 The degree of stationarity $DS(\omega)$ is often used to investigate the stationarity and periodicity of
 27 the data, it is defined as:

$$1 \quad DS(\omega) = \frac{1}{T} \int_0^T \left(1 - \frac{H(\omega, t)}{h(\omega)/T}\right)^2 dt, \quad (11)$$

2 where T is the entire time span.

3 The volatility ~~which~~ $V(t, T)$ is defined as the ratio of the sum of certain IMF components $S_h(t)$ to
 4 the original signal $S(t)$, ~~here~~. Here we use the summation of residual and all the IMFs but the
 5 first one as $S_h(t)$:

$$6 \quad V(t, T) = \frac{S_h(t)}{S(t)} = \frac{\sum_{j=2}^n c_j(t) + r(t)}{S(t)}, \quad (12)$$

7 where n is the number of IMFs.

8 **2.5 The gap-filling of the monthly average ozone data**

9 To perform the HHT analysis, a complete, even-spaced dataset is required. Hence we need to
 10 fill the gaps in the monthly average surface ozone mixing ratio data. ~~The location of the gaps~~
 11 ~~can be seen in b. It can be noted that gaps could~~ In our monthly ozone time series, gaps of one
 12 to six months can be found in 1997, 1998, 1999 and 2002. If the gap is small and occurs in
 13 between the ozone seasonal low and peak value, then a spline interpolation would suffice.
 14 However, this is not the case for some gaps. In 1997 and 1998, the gaps ~~occurred~~ occurred during
 15 summertime, when the seasonal peak of ozone mixing ratio ~~should~~ would be ~~highest~~ expected.
 16 In 2002, the gap ~~continues~~ continued on to winter, when the ozone mixing ratio should be lowest.
 17 A simple spline interpolation would underestimate the seasonal peak value and overestimate
 18 the seasonal low. Hence, we applied the following method to fill the gaps.

19 First, the monthly mean ozone timeseries ~~during from~~ 1994 to 2013, ~~as is shown in b~~, is shaped
 20 into an array $O_3(i, j)$ of the size [20 years \times 12 months], where $i=1994, \dots, 2013$ and $j=1, \dots, 12$.

21 The gaps in $O_3(i, j)$ are filled by applying a spline interpolation on each row of the array:

$$22 \quad O_{3, spline}(1994, \dots, 2013, j) = spline(O_3(1994, \dots, 2013, j)), j = 1, \dots, 12 \quad (13)$$

23 In this way, both the average value of ozone mixing ratio at a certain month and the overall
 24 ozone variation trend will be considered. A complete dataset of average monthly ozone mixing
 25 ratio can then be recreated by using interpolated data only on months of missing observation
 26 data:

$$27 \quad O_{3, complete} = \begin{cases} O_{3, spline}, & \text{missing } O_3 \\ O_3, & \text{existing } O_3 \end{cases} \quad (14)$$

1 ~~The result is displayed in a, with the original data in solid lines and interpolated data in dashed~~
2 ~~lines.~~ Our method could yield a reasonable interpolated timeseries with both seasonal low and
3 peak values occurring at the right time of year.

4 **3 Results and Discussion**

5 **3.1 Season-diurnal variation characteristics of ozone**

6 The average season-diurnal variation of surface ozone during 1994 ~~to~~ 2013 is displayed in
7 Figure 2- ~~with the monthly average local times associated with the diurnal minimum ozone and~~
8 ~~maximum zonal wind.~~ The seasonal maximum ozone occurs during summer, with an average
9 peak in June-July, while the minimum is found in winter (Figure 3a), which will be discussed
10 in detail in Section 3.2.

11 Daily maximum ozone usually occurs during nighttime, while the daily minimum ozone is
12 found around noontime, on average at 12 am, Beijing Local Time (Figure 3c). Ma et al. (2002b)
13 suggest that the WLG station is mostly influenced by boundary layer (BL) air that is brought
14 up through an upslope flow during the day, while a downslope flow brings down free
15 tropospheric (FT) air during the night. The BL air masses are typically characterised by lower
16 ozone mixing ratios in comparison with FT air masses, hence the occurrence of the daily ozone
17 minimum value indicates the time when the BL is fully developed and the air within is well
18 mixed.

19 From Figure 3b) it can be denoted that, the occurrence time of the daily minimum ozone mixing
20 ratio (red dots) shows a significant seasonal variation similar to that of the maximum zonal
21 wind velocity (white dots), with the former occurring 1-2 hours earlier than the later. Due to
22 the seasonal variation of the development of the boundary layer, the daily minimum ozone
23 should occur earlier in the day during warm seasons and later in the day during cold seasons.

24 This phenomenon can indeed be confirmed by Figure 3b), however, the ozone minimum of
25 June-August seems to occur later than expected. This phenomenon ~~couldis not been foundseen~~
26 in the season-diurnal variation of horizontal or vertical wind speeds, ~~thusindicating that~~ it is not
27 caused by boundary layer development. A possible explanation might be that the photochemical
28 production of ozone was enhanced at early noon during summertime, leading to a delayed
29 noontime minimum. The in-situ ozone production/destruction in different seasons is not well
30 quantified at the moment. Previous studies focused on modelling the photochemical net
31 production in spring and summer and reached to controversial conclusions (Ma et al.,

1 2002b; Wang et al., 2015). Hence there is a need for more investigation into the cause for such
2 a phenomenon.

4 **3.2 Season-annual variation characteristics of ozone**

5 Figure 4 displays the season-annual variation of surface ozone during 1994 to 2013. Again,
6 the ozone mixing ratio peaks in summer and is lowest during winter (Fig. 4b), with an average
7 seasonal peak occurring in June during 1994 to 2013 (Fig. 4c). Previous studies reported the
8 same seasonal ozone pattern, but attributed the summertime peak to different causes, e.g., more
9 frequent STE events (Ding and Wang, 2006; Tang et al., 2011), enhanced vertical convection
10 (Ma et al., 2005), long-range transport from eastern-central China, central-southern Asia or
11 even Europe during summer (Zhu et al., 2004) and stronger cross boundary transport and
12 vertical convection during the East Asian summer monsoon season (Yang et al., 2014). From
13 Fig. 2c it can be noted that nighttime subsiding wind is indeed strongest in summer, which
14 supports the hypothesis of downward transport of ozone. Zheng et al. (2011) argue that STE
15 reaches maximum strength in spring and shows a decline in late spring based on $^{10}\text{Be}/^7\text{Be}$
16 measurements, indicating that the continuous ozone increase in summer is caused by the
17 photochemical production. The seasonal variation of STE and its impact on surface ozone will
18 be handled in the second part of our study.

19 The long-term variation of the annual average ozone exhibits a clear increasing trend (Fig. 4a).
20 A 2-4 year cycle seems to exist within the long-term variation of surface ozone. Previous study
21 has shown that there is a quasi-biannual oscillation (QBO) within the total ozone column
22 density over the Tibetan Plateau, which is in antiphase with the QBO of the tropical
23 stratospheric winds, exhibiting a 29-month cycle (Ji et al., 2001). The influence of the QBO
24 could extend to WLG station at the 3.8 km altitude via STE. Thus, ~~the~~ surface ozone at WLG
25 might also have a QBO with a similar periodicity, which is related to that of the total ozone
26 column. The periodicity within the surface ozone data will be further discussed in sect. 3.4.

27 **3.3 Long-term variation trends of ozone**

28 The trends of monthly average all-day, daytime and nighttime ozone during 1994 to 2013 are
29 displayed in Figs. 5a1-c1, respectively. Ozone data in Figs. 5b1 and 5c1 are the subsets of data
30 from the daytime and nighttime ranges determined in Section 2.2 based on the zonal wind

1 information. The increase in surface ozone in the past two decades is evident in all three data
2 subsets, with a slightly stronger increase in the nighttime data. The linear trends for all-day,
3 daytime and nighttime ozone mixing ratios reached 2.5 ± 1.7 , 2.4 ± 1.6 and 2.8 ± 1.7 ppbv $10a^{-1}$,
4 respectively, while the Kendall slopes reached 1.8, 1.7, 1.9 ppbv $10a^{-1}$, respectively. The
5 Kendall slope is smaller than the linear regression slope, mainly because the linear regression
6 method ~~does not consider~~ is influenced by the seasonality within the data. However, both
7 methods yielded statistically significant increasing trends.

8 To further investigate the trend ~~in~~ of ozone in different seasons, the trend of seasonal average
9 ozone during 1994 ~~to~~ – 2013 was calculated and are shown in Figs. 5a-c (2-5). After eliminating
10 the seasonality in the data, the linear least squares fitting slopes and Kendall's ~~slopes~~ slopes
11 yielded very similar results, thus ~~we only listed~~ the linear slopes and p-values are listed in Table
12 1. The strongest increase in surface ozone was found in autumn (SON), followed by spring
13 (MAM), respectively reaching 2.8 ± 1.1 and 2.4 ± 1.1 ppbv $10a^{-1}$ in the seasonal average of all-
14 day ozone mixing ratios. In comparison, summer (JJA) and winter (DJF) both showed much
15 weaker increasing trends, with rates of 1.5 ± 1.9 and 1.4 ± 0.9 ppbv $10a^{-1}$, respectively, amongst
16 which ~~and~~ the summertime trend could not even reach a confidence level of 95%. In summer
17 the daytime increasing rate is significantly lower than the nighttime one, respectively reaching
18 0.7 ± 1.8 and 2.2 ± 2.0 ppbv $10a^{-1}$. The nighttime slope reached the confidence level of 95%,
19 while the daytime slope is statistically insignificant.

20 ~~Past~~ Previous investigations on the air-mass origin of WLG have shown that WLG is mostly
21 governed by western and northwestern air-masses, air-masses coming from the eastern sector
22 takes up only 2%, 5% and 8% in winter, spring and autumn, respectively (Zhang et al., 2011).
23 However, ~~in summer there is~~ a significant percentage (30%) of air-masses ~~coming~~ come from
24 the eastern direction during summertime. Since the two major cities in the vicinity of WLG are
25 both in the east, summertime is believed to be the season in which WLG is most influenced by
26 nearby anthropogenic activities. From the diurnal variation of the horizontal wind speeds (Figs.
27 2a-b) it can be discerned that daytime winds are weak northern winds, while nighttime winds
28 are rather strong north-easterly winds, which are more in favour of transporting anthropogenic
29 pollution to WLG.

30 As already mentioned before in Section 3.2, some ~~research~~ researchers believe that STE is also
31 most frequent in summer at WLG (Ding and Wang, 2006). During the night the WLG site is
32 governed by downwards winds, which may bring down air with high ozone mixing ratios from

1 above. Hence, an increase in the frequency of STE events would also result in increasing
2 nighttime ozone mixing ratios in summer. Whether it is anthropogenic activities or rather
3 meteorological factors, that has led to the distinct daytime and nighttime ozone variation slopes
4 in summer, still needs further investigations and will be discussed in Part 2 of our study.

5 The seasonal peak of the Northern Hemisphere background ozone typically occurs in spring,
6 which is believed to be the result of enhanced photochemical production in spring (Monks,
7 2000;Vingarzan, 2004). Unlike other sites in the Northern Hemisphere, the seasonal ozone peak
8 at WLG occurs during summer. However, the largest increase in ozone mixing ratio was found
9 in autumn rather than in summer. Lin et al. (2014) also reported significant increasing ozone
10 trends in autumn rather than spring at the Mauna Loa Observatory in Hawaii in the past 4
11 decades and attributed this phenomenon to strengthened ozone-rich air flows from Eurasia. The
12 ~~reason why fact that~~ we observed the largest ozone increase in ~~ozone levels during~~ autumn ~~also~~
13 ~~needs further exploration and is possibly linked to changes in atmospheric circulation. Details~~
14 will be ~~handled~~discussed in ~~Part 2~~the companion paper.

15 Here we present a comparison between the seasonal ozone variation trends of all the high
16 altitude (>1200 m asl) sites in the northern hemisphere (Table 2). The stations have been sorted
17 by latitude. The low latitude sites, Mauna Loa and Izaña, both show increasing trends (3.1 ± 0.7
18 and 1.4 ± 0.5 ppbv $10a^{-1}$) during 1991 ~~to~~ 2010 (Oltmans et al., 2013). Lin et al. (2014) ~~suggested~~
19 ~~that, in compared the ozone levels at the Mauna Loa site in Hawaii during~~ the period of 1995
20 to 2011 ~~in comparison with the period to that~~ of 1980 to 1995, ~~the Mauna Loa site in Hawaii~~
21 ~~displays and discovered a~~ strong ~~increasing ozone mixing ratios~~increase during summer and
22 autumn. The mid-latitude stations exhibit inconsistent trends. Significantly positive trends were
23 detected in the Rocky Mountains, USA (3.3 ± 0.5 ppbv $10a^{-1}$, Oltmans et al., 2013) and at
24 Jungfrauoch, Switzerland (3.2 ± 1.8 ppbv $10a^{-1}$, Cui et al., 2011). Tarasova et al. (2009) found
25 evidence for increased stratospheric contribution to surface ozone at Jungfrauoch. The
26 strongest increase at Jungfrauoch was detected in winter; ~~and~~ and the weakest in summer. Gilge et
27 al. (2010) also reported increased wintertime ozone at two other ~~two~~ alpine sites in central
28 Europe during 1995-2007. Lin et al. (2015b) reported ~~that springtime free tropospheric ozone~~
29 ~~displays~~ an increasing trend of 0.31 ± 0.21 ppbv a^{-1} in springtime free-tropospheric ozone over
30 western North America during 1995-2014, however, by shutting ~~of~~ North American emissions
31 in the model and focusing on the subset of ozone associated with Asian influence (also possibly
32 mixed with stratospheric intrusions), the background ozone revealed a more significant

1 increasing rate of 0.55 ± 0.14 ppbv a^{-1} during 1992-2012. No significant trends were found at
2 Pinadale, USA and Zugspitze, Germany. Negative trends were revealed at Kislovodsk, Russia
3 (-3.7 ± 1.4 ppbv $10a^{-1}$, Tarasova et al., 2009) and Whiteface, USA (-2.2 ± 0.6 ppbv $10a^{-1}$,
4 Oltmans, 2013). Tarasova et al. (2009) attributed the strong decrease in ozone in Kislovodsk to
5 control measures of Europe and the breakdown of the former USSR. Both the strong increasing
6 and decreasing trends at Jungfraujoch and Kislovodsk were mostly caused by the variation in
7 ozone mixing ratios in the 1990s. The positive trend at Jungfraujoch during the 1990s was
8 strongest in spring and weakest in summer and autumn, while the reduction at Kislovodsk was
9 strongest in summer and weaker in autumn and winter (Tarasova et al., 2009). After 2000, the
10 eastern U.S. was revealed significant decrease due to the implementation of NO_x emission
11 control measures, while ozone mixing ratios at the other sites in the northern mid-latitudes have
12 entered a steady stage with either slow or no growth (Tarasova et al., 2009; Oltmans et al., 2013).
13 In comparison, WLG shows a continuous rise of ozone mixing ratio throughout the past two
14 decades and the most significant positive trends appear in autumn and spring, unlike the other
15 mid-latitude stations. The cause effor this phenomenon still needs further exploration and will
16 be discussed in Part 2.

17 **3.4 Hilbert-Huang Spectral Analysis of surface ozone at WLG**

18 The long-term variation of surface ozone may be the result fromof changes in emissions of
19 ozone precursors, but may also be caused by year-to-year fluctuations or multiyear oscillations
20 of climate conditions. All the related factors have different periodicities, which is why the
21 variation of ozone is highly non-linear. To unravel the potential oscillations on different time
22 scales in the ozone timeseries, we performed an HHT analysis on the ozone data from WLG
23 using the method given in Section 2.4. The result of the EMD is shown in Fig. described in
24 Section 2.4. Our effort is the first time that the HHT method has been applied in the analysis of
25 atmospheric composition data. The first step of this analysis was the EMD filtering of the
26 timeseries of monthly average ozone mixing ratio. The results of the EMD are shown in Fig. 6.
27 The monthly average ozone signal could be decomposed into 5 IMFs with different
28 characteristic time scales. The lowest order IMF (c1) shows an oscillation with the highest
29 frequency. The second IMF (c2) shows the seasonal variation in the ozone signal. C3 reveals
30 3-4 year oscillations, c4 shows 7 year oscillations and the highest order IMF (c5 in Fig. 6f)
31 shows the longest oscillations pattern, with a quasi-10-year periodicity.

1 ~~Segmentations is~~ A segmentation analysis was performed by finding the local extrema of c5.
2 The total time span could be separated into 4 segments, as indicated by the dotted lines in Fig.
3 6a. The slope of the segments of c5 can indicate whether the value is increasing or declining.
4 To determine the significance of the trend, the modified Mann-Kendall trend test ~~is was~~
5 performed on each segment and the results are given in Table 3. The first segment ~~lasts lasted~~ 3
6 years (from Aug. 1994 to Jun. 1997) and ~~reveals revealed~~ no significant trend ($z=1.42$), with an
7 increasing slope of $2.7 \text{ ppbv } 10\text{a}^{-1}$. The second segment ~~lasts lasted~~ for 5 years (from Jul. 1997
8 to May 2002) and ~~displays displayed~~ a significant upward trend ($z=3.66$). ~~The), with an~~
9 increasing slope ~~reaches of~~ $4.2 \text{ ppbv } 10\text{a}^{-1}$. Afterwards the ~~increasing speed increase~~ of ~~the~~ ozone
10 mixing ~~ratios ratio~~ at WLG ~~slows slowed~~ down in segment 3, lasting 6 years (from Jun. 2002 to
11 Apr. 2008), with a variation slope of $3.0 \text{ ppbv } 10\text{a}^{-1}$; ~~however, the increasing trend~~
12 ~~remains remained~~ significant ($z=3.57$). In the last segment, ~~which starts in (from~~ May 2008 ~~and~~
13 ~~ends into the end of~~ Jul. 2013; ~~),~~ the significant upward trend ~~continues continued~~ ($z=3.65$) with
14 a larger increasing slope ($3.6 \text{ ppbv } 10\text{a}^{-1}$) than that in segment 3.

15 Overall, surface ozone mixing ratio at WLG ~~has been rising increased~~ continuously ~~since from~~
16 1997 ~~to 2013~~. Figure 7a shows the anomaly of the interpolated monthly average ozone during
17 1994 ~~to 2013~~, its overall variation trend (represented by c5+r in Fig. 6) and its variation on a
18 scale of 7-year or longer (represented by c4+c5+r in Fig. 6). The corresponding variation slopes
19 of the overall variation trend and the 7-year or longer variation is depicted in Fig. 7b. The
20 overall variation trend confirms the continuous increase since Jan. 1997. The two largest slopes
21 are respectively detected in May 2000 and Oct. 2010. The 7-year or longer trend line displays
22 a rise in ozone after Aug. 1996, which reaches a maximum increasing speed in Sep. 2003.
23 Afterwards, the increase slows down and turns into a decreasing trend in Sep. 2005. After Jan.
24 2009, ozone mixing ratios went up again, reaching a maximum increasing speed in Dec. 2010.

25 The Hilbert Energy Spectrum is depicted in Fig. 8d, along with the volatility, instantaneous
26 energy (IE) and the degree of stationarity (DS) (Figs. 8b, ~~e, e8c and 8e~~). Both the volatility and
27 the IE reflect the variation of energy with time. Compared to the mean IE, which represents the
28 temporal variation of the frequency averaged energy, volatility rather focuses on the ratio of the
29 variation of certain signals to the total signal. Peaks in the mean IE could be found in 1994-
30 1995, 2000-2001, 2003, 2008 and 2013; ~~(Fig. 8c)~~, which ~~corresponds correspond~~ to the high
31 ozone mixing ratio values in the data. High values of volatility were found around 2003, 2008

带格式的

1 and 2012; (Fig. 8b), which mostly agree with those of the IE. The cause for these high anomalies
2 still needs to be investigated upon.

3 The DS corresponding to each frequency, as displayed in Fig. 8e, can provide information on
4 the underlying periodicity within the original signal. The smaller the DS is, the more stationary
5 the data is at this frequency. ~~The lower~~ Lower DS values are observed in the low frequency part.
6 A dip-down at the frequencies between 0.08 and 0.12 ~~could~~ can be found, which corresponds to
7 the annual cycle of ozone. Other dip-downs are found at even lower frequencies, corresponding
8 to 2.5a, 3.5a, 7a and 11a cycles. Among all the known atmospheric factors that have an impact
9 on the ozone mixing ratio at WLG, QBO ~~has a quasi 2 year cycle~~, ENSO ~~bears a 2 to 7 year~~
10 ~~cycle and solar activities vary with a 11 year cycle. The combined effect of QBO and ENSO,~~
11 ~~etc.,~~ could be responsible for ~~the 2.5a or 3.5a periodicity as suggested by the DS. these~~
12 ~~periodicities.~~ Further investigations of these periodicities and related factors will be carried out
13 in Part 2.

14 Overall, the HHT analysis was able to detect variations in surface ozone trends during different
15 periods, and was successful in finding the anomalies and periodicities within the data. Results
16 of this analysis can further facilitate the attribution of the variations of surface ozone at WLG
17 to the influencing factors, which will be discussed in the companion paper.

18 **4 Summary**

19 In this paper we present the characteristics, trends and periodicity of surface ozone mixing ratio
20 at a global baseline GAW station in the eastern Tibetan Plateau region (Mt. Waliguan) during
21 the past two decades. The trends and periodicity of ozone were investigated using a modified
22 Mann-Kendall test and an adaptive method (Hilbert Huang Transform) that is suited for
23 analysing non-stationary and non-linear natural processes.

24 ~~Results reveal that While confirming the reported diurnal and seasonal characteristics of surface~~
25 ~~ozone at WLG is higher during the night and lower during, our study reveals a relationship~~
26 ~~between the day, because the station is under the control of ozone rich free tropospheric air~~
27 ~~during the night and boundary layer air during the day due to seasonality in~~ mountain-valley
28 ~~breeze. Ozone displays a and the seasonal shift in the occurrence time of daily maximum in~~
29 ~~summer and minimum in winter, which is probably caused by enhanced stratosphere-to-~~
30 ~~troposphere exchange events and/or by tropospheric photochemistry. Analysis suggests that~~
31 ~~there is a ozone at the site. Based on this relationship, season-diurnal cycle in the three-~~
32 ~~dimensional winds on top of Mt. Waliguan. This allows for defining well-~~

1 ~~developmentdependent~~ daytime and nighttime ~~ranges that change from month to month.~~ Trends
2 ~~of surface ozone were calculated for the data subsets of the periods are defined for separately~~
3 ~~analysing the~~ daytime and nighttime ~~as well as for all day in different seasons~~ trends of surface
4 ~~ozone.~~ Both daytime and nighttime surface ozone has been significantly increasing at WLG.
5 Autumn and spring revealed the largest increase rates, while summer and winter showed
6 relatively weaker increases. A significant daytime and nighttime difference in trend could only
7 be found in summer, where nighttime ozone was significantly increasing and daytime ozone
8 ~~bears no significant trend. Summer is the season during which WLG is mostly influenced by~~
9 ~~airmasses from the eastern sector. Whether anthropogenic activities in the two nearest major~~
10 ~~cities in the eastern sector have impacts on the trend of summertime ozone still needs further~~
11 ~~exploration.~~

12 ~~had no significant trend.~~ Results of the HHT spectral analysis confirm the increasing trends in
13 surface ozone mixing ratio and ~~could~~ further identify four different stages with different
14 increasing rates. The overall trend indicates that the largest increase occurred around May 2000
15 and Oct. 2010. The ozone signal was also decomposed into five intrinsic mode functions with
16 different time scales. ~~A 2-4 year, 7 year and 11 year periodicity was periodicities were~~ found
17 within the data, the cause of which still needs further investigation.

18 The results obtained in this work are ~~very~~ valuable for related climate and environment change
19 assessments of western China and surrounding areas, and ~~for~~ can be used in the validation of
20 chemical-climate models. As WLG is a high altitude mountain-top site in a remote region,
21 measurements of surface ozone and other species can well represent a large scale situation.
22 Previous ~~t~~ air mass origin ~~studies~~ and modelling studies (Zhang et al., 2011; Li et al., 2014)
23 suggest that WLG is mostly under the influence of transport from the north-west direction,
24 hence the upward trend in ozone might be ~~a reflectance upon an~~ an indication of impact of transport
25 from ~~Europe that direction.~~ Since ~~Easterneastern~~ China is in the downwind direction, our
26 results imply that under rising background ozone conditions, even more effort needs to be put
27 in reducing ozone precursors. In the second part of our study, influencing factors or potential
28 causes of the ~~impact of different air mass origins and the observed~~ long-term ~~variation trends~~
29 of ~~their occurrence frequencies on the~~ surface ozone ~~mixing ratio and its trend~~ at WLG will be
30 ~~shown. The anthropogenic impact of the nearest major population centers on the ozone trend~~
31 ~~will be addressed and~~ discussed. ~~The long-term variation of STE and its link to surface ozone~~
32 ~~at WLG will be displayed. The possible connection of changes in atmospheric circulation~~

带格式的
带格式的

1 ~~oscillations and solar activities with the inner annual and periodical variations of ozone at WLG~~
2 ~~will be studied.~~

4 **Acknowledgements**

5 We thank all operators of the Mt. Waliguan Baseline Station for their excellent routine work.
6 We appreciate WMO/GEF, WMO/GAW, Canada/AES, and Swiss/WCC-Empa for funding and
7 technical support. This work is supported by China Special Fund for Meteorological Research
8 in the Public Interest (No. GYHY201106023), ~~China Special Fund for~~ Environmental
9 Protection Public Welfare Scientific Research in Project, Ministry of Environmental Protection
10 of the Public Interest (People's Republic of China (Grant No. 201509002), the Basic Research
11 Fund of CAMS (No. 2013Z005) and the Natural Science Foundation of China (No. 41505107
12 and 21177157).

1 References

- 2 Ambrose, J. L., Reidmiller, D. R., and Jaffe, D. A.: Causes of high O₃ in the lower free
3 troposphere over the Pacific Northwest as observed at the Mt. Bachelor Observatory,
4 Atmospheric Environment, 45, 5302-5315, <http://dx.doi.org/10.1016/j.atmosenv.2011.06.056>,
5 2011.
- 6 Bonasoni, P., Evangelisti, F., Bonafe, U., Ravegnani, F., Calzolari, F., Stohl, A., Tositti, L.,
7 Tubertini, O., and Colombo, T.: Stratospheric ozone intrusion episodes recorded at Mt. Cimone
8 during the VOTALP project: case studies, Atmospheric Environment, 34, 1355-1365,
9 [http://dx.doi.org/10.1016/S1352-2310\(99\)00280-0](http://dx.doi.org/10.1016/S1352-2310(99)00280-0), 2000.
- 10 Cooper, O. R., Parrish, D. D., Stohl, A., Trainer, M., Nedelec, P., Thouret, V., Cammas, J. P.,
11 Oltmans, S. J., Johnson, B. J., Tarasick, D., Leblanc, T., McDermid, I. S., Jaffe, D., Gao, R.,
12 Stith, J., Ryerson, T., Aikin, K., Campos, T., Weinheimer, A., and Avery, M. A.: Increasing
13 springtime ozone mixing ratios in the free troposphere over western North America, Nature,
14 463, 344-348, [10.1038/nature08708](https://doi.org/10.1038/nature08708), 2010.
- 15 Cui, J., Pandey Deolal, S., Sprenger, M., Henne, S., Staehelin, J., Steinbacher, M., and Nédélec,
16 P.: Free tropospheric ozone changes over Europe as observed at Jungfraujoch (1990–2008): An
17 analysis based on backward trajectories, Journal of Geophysical Research: Atmospheres, 116,
18 n/a-n/a, [10.1029/2010JD015154](https://doi.org/10.1029/2010JD015154), 2011.
- 19 Ding, A., and Wang, T.: Influence of stratosphere-to-troposphere exchange on the seasonal
20 cycle of surface ozone at Mount Waliguan in western China, Geophysical Research Letters, 33,
21 L03803, [10.1029/2005GL024760](https://doi.org/10.1029/2005GL024760), 2006.
- 22 Ding, A. J., Wang, T., Thouret, V., Cammas, J. P., and Nédélec, P.: Tropospheric ozone
23 climatology over Beijing: analysis of aircraft data from the MOZAIC program, Atmos. Chem.
24 Phys., 8, 1-13, [10.5194/acp-8-1-2008](https://doi.org/10.5194/acp-8-1-2008), 2008.
- 25 El-Askary, H., Sarkar, S., Chiu, L., Kafatos, M., and El-Ghazawi, T.: Rain gauge derived
26 precipitation variability over Virginia and its relation with the El Nino southern oscillation,
27 Advances in Space Research, 33, 338-342, [http://dx.doi.org/10.1016/S0273-1177\(03\)00478-2](http://dx.doi.org/10.1016/S0273-1177(03)00478-2),
28 2004.
- 29 Gilge, S., Plass-Duelmer, C., Fricke, W., Kaiser, A., Ries, L., Buchmann, B., and Steinbacher,
30 M.: Ozone, carbon monoxide and nitrogen oxides time series at four alpine GAW mountain
31 stations in central Europe, Atmos. Chem. Phys., 10, 12295-12316, [10.5194/acp-10-12295-2010](https://doi.org/10.5194/acp-10-12295-2010),
32 2010.
- 33 Hamed, K. H., and Ramachandra Rao, A.: A modified Mann-Kendall trend test for
34 autocorrelated data, Journal of Hydrology, 204, 182-196, [http://dx.doi.org/10.1016/S0022-](http://dx.doi.org/10.1016/S0022-1694(97)00125-X)
35 [1694\(97\)00125-X](http://dx.doi.org/10.1016/S0022-1694(97)00125-X), 1998.
- 36 Helsel, D. R., Mueller, D. K., and Slack, J. R.: Computer program for the Kendall family of
37 trend tests: U.S. Geological Survey Scientific Investigations Report 2005-5275, 4p.b,
38 <http://pubs.usgs.gov/sir/2005/5275/pdf/sir2005-5275.pdf>, 2006.
- 39 Huang, N. E., Shen, Z., Long, S. R., Wu, M. C., Shih, H. H., Zheng, Q., Yen, N.-C., Tung, C.
40 C., and Liu, H. H.: The empirical mode decomposition and the Hilbert spectrum for nonlinear
41 and non-stationary time series analysis, Proceedings of the Royal Society of London A:
42 Mathematical, Physical and Engineering Sciences, 1998, 903-995,

- 1 Huang, N. E., Wu, M.-L. C., Long, S. R., Shen, S. S., Qu, W., Gloersen, P., and Fan, K. L.: A
2 confidence limit for the empirical mode decomposition and Hilbert spectral analysis,
3 Proceedings of the Royal Society of London A: Mathematical, Physical and Engineering
4 Sciences, 2003, 2317-2345,
- 5 Huang, N. E., and Wu, Z.: A review on Hilbert-Huang transform: Method and its applications
6 to geophysical studies, Reviews of Geophysics, 46, RG2006, 10.1029/2007RG000228, 2008.
- 7 Huang, N. E.: Hilbert-Huang transform and its applications, World Scientific, 2014.
- 8 IPCC: Climate Change 2013: The Physical Science Basis. Contribution of Working Group I to
9 the Fifth Assessment Report of the Intergovernmental Panel on Climate Change, Cambridge
10 Univ. Press, Cambridge, United Kingdom and New York, NY, USA, 1535, 2013.
- 11 Ji, C. P., Zou, H., and Zhou, L. B.: QBO Signal in Total Ozone Over the Tibet, Climatic and
12 Environmental Research, 6, 416-424, 2001.
- 13 Jia, S., Xu, X., Lin, W., Wang, Y., He, X., and Zhang, H.: Increased mixing ratio of surface
14 ozone by nighttime convection process over the North China Plain, Journal of Applied
15 Meteorological Science, 26, 280-290, 2015.
- 16 Kendall, M. G.: Rank Correlation Methods, Charles Griffin, London, 1955.
- 17 Lal, S., Venkataramani, S., Chandra, N., Cooper, O. R., Brioude, J., and Naja, M.: Transport
18 effects on the vertical distribution of tropospheric ozone over western India, Journal of
19 Geophysical Research: Atmospheres, 2014JD021854, 10.1002/2014JD021854, 2014.
- 20 Langford, A. O., Aikin, K. C., Eubank, C. S., and Williams, E. J.: Stratospheric contribution to
21 high surface ozone in Colorado during springtime, Geophysical Research Letters, 36, n/a-n/a,
22 10.1029/2009GL038367, 2009.
- 23 Langford, A. O., Senff, C. J., Alvarez Ii, R. J., Brioude, J., Cooper, O. R., Holloway, J. S., Lin,
24 M. Y., Marchbanks, R. D., Pierce, R. B., Sandberg, S. P., Weickmann, A. M., and Williams, E.
25 J.: An overview of the 2013 Las Vegas Ozone Study (LVOS): Impact of stratospheric intrusions
26 and long-range transport on surface air quality, Atmospheric Environment, 109, 305-322,
27 <http://dx.doi.org/10.1016/j.atmosenv.2014.08.040>, 2015.
- 28 Lefohn, A. S., Wernli, H., Shadwick, D., Oltmans, S. J., and Shapiro, M.: Quantifying the
29 importance of stratospheric-tropospheric transport on surface ozone concentrations at high- and
30 low-elevation monitoring sites in the United States, Atmospheric Environment, 62, 646-656,
31 <http://dx.doi.org/10.1016/j.atmosenv.2012.09.004>, 2012.
- 32 Lelieveld, J., and Dentener, F. J.: What controls tropospheric ozone?, Journal of Geophysical
33 Research: Atmospheres, 105, 3531-3551, 10.1029/1999JD901011, 2000.
- 34 Li, X., Liu, J., Mauzerall, D. L., Emmons, L. K., Walters, S., Horowitz, L. W., and Tao, S.:
35 Effects of trans-Eurasian transport of air pollutants on surface ozone concentrations over
36 Western China, Journal of Geophysical Research: Atmospheres, 119, 12,338-312,354,
37 10.1002/2014JD021936, 2014.
- 38 Lin, M., Fiore, A. M., Cooper, O. R., Horowitz, L. W., Langford, A. O., Levy, H., Johnson, B.
39 J., Naik, V., Oltmans, S. J., and Senff, C. J.: Springtime high surface ozone events over the
40 western United States: Quantifying the role of stratospheric intrusions, Journal of Geophysical
41 Research: Atmospheres, 117, n/a-n/a, 10.1029/2012JD018151, 2012a.
- 42 Lin, M., Fiore, A. M., Horowitz, L. W., Cooper, O. R., Naik, V., Holloway, J., Johnson, B. J.,
43 Middlebrook, A. M., Oltmans, S. J., Pollack, I. B., Ryerson, T. B., Warner, J. X., Wiedinmyer,

1 C., Wilson, J., and Wyman, B.: Transport of Asian ozone pollution into surface air over the
2 western United States in spring, Journal of Geophysical Research: Atmospheres, 117, n/a-n/a,
3 10.1029/2011JD016961, 2012b.

4 Lin, M., Horowitz, L. W., Oltmans, S. J., Fiore, A. M., and Fan, S.: Tropospheric ozone trends
5 at Mauna Loa Observatory tied to decadal climate variability, Nature Geosci, 7, 136-143,
6 10.1038/ngeo2066, 2014.

7 Lin, M., Fiore, A. M., Horowitz, L. W., Langford, A. O., Oltmans, S. J., Tarasick, D., and
8 Rieder, H. E.: Climate variability modulates western US ozone air quality in spring via deep
9 stratospheric intrusions, Nat Commun, 6, 10.1038/ncomms8105, 2015a.

10 Lin, M., Horowitz, L. W., Cooper, O. R., Tarasick, D., Conley, S., Iraci, L. T., Johnson, B.,
11 Leblanc, T., Petropavlovskikh, I., and Yates, E. L.: Revisiting the evidence of increasing
12 springtime ozone mixing ratios in the free troposphere over western North America,
13 Geophysical Research Letters, n/a-n/a, 10.1002/2015GL065311, 2015b.

14 Logan, J. A., Staehelin, J., Megretskaya, I. A., Cammas, J. P., Thouret, V., Claude, H., De
15 Backer, H., Steinbacher, M., Scheel, H. E., Stübi, R., Fröhlich, M., and Derwent, R.: Changes
16 in ozone over Europe: Analysis of ozone measurements from sondes, regular aircraft (MOZAIC)
17 and alpine surface sites, Journal of Geophysical Research: Atmospheres, 117, D09301,
18 10.1029/2011JD016952, 2012.

19 Lundquist, J. K.: Intermittent and Elliptical Inertial Oscillations in the Atmospheric Boundary
20 Layer, Journal of the Atmospheric Sciences, 60, 2661-2673, 10.1175/1520-
21 0469(2003)060<2661:IAEIOI>2.0.CO;2, 2003.

22 Ma, J., Liu, H., and Hauglustaine, D.: Summertime tropospheric ozone over China simulated
23 with a regional chemical transport model 1. Model description and evaluation, Journal of
24 Geophysical Research: Atmospheres, 107, ACH 27-21-ACH 27-13, 10.1029/2001JD001354,
25 2002a.

26 Ma, J., Tang, J., Zhou, X., and Zhang, X.: Estimates of the Chemical Budget for Ozone at
27 Waliguan Observatory, Journal of Atmospheric Chemistry, 41, 21-48,
28 10.1023/A:1013892308983, 2002b.

29 Ma, J., Zheng, X., and Xu, X.: Comment on “Why does surface ozone peak in summertime at
30 Waliguan?” by Bin Zhu et al, Geophysical Research Letters, 32, n/a-n/a,
31 10.1029/2004GL021683, 2005.

32 Ma, J., Lin, W. L., Zheng, X. D., Xu, X. B., Li, Z., and Yang, L. L.: Influence of air mass
33 downward transport on the variability of surface ozone at Xianggelila Regional Atmosphere
34 Background Station, southwest China, Atmos. Chem. Phys., 14, 5311-5325, 10.5194/acp-14-
35 5311-2014, 2014.

36 Monks, P. S.: A review of the observations and origins of the spring ozone maximum,
37 Atmospheric Environment, 34, 3545-3561, [http://dx.doi.org/10.1016/S1352-2310\(00\)00129-1](http://dx.doi.org/10.1016/S1352-2310(00)00129-1),
38 2000.

39 Oltmans, S. J., Lefohn, A. S., Harris, J. M., Galbally, I., Scheel, H. E., Bodeker, G., Brunke, E.,
40 Claude, H., Tarasick, D., Johnson, B. J., Simmonds, P., Shadwick, D., Anlauf, K., Hayden, K.,
41 Schmidlin, F., Fujimoto, T., Akagi, K., Meyer, C., Nichol, S., Davies, J., Redondas, A., and
42 Cuevas, E.: Long-term changes in tropospheric ozone, Atmospheric Environment, 40, 3156-
43 3173, <http://dx.doi.org/10.1016/j.atmosenv.2006.01.029>, 2006.

1 Oltmans, S. J., Lefohn, A. S., Shadwick, D., Harris, J. M., Scheel, H. E., Galbally, I., Tarasick,
2 D. W., Johnson, B. J., Brunke, E. G., Claude, H., Zeng, G., Nichol, S., Schmidlin, F., Davies,
3 J., Cuevas, E., Redondas, A., Naoe, H., Nakano, T., and Kawasato, T.: Recent tropospheric
4 ozone changes – A pattern dominated by slow or no growth, Atmospheric Environment, 67,
5 331-351, <http://dx.doi.org/10.1016/j.atmosenv.2012.10.057>, 2013.

6 Parrish, D. D., Law, K. S., Staehelin, J., Derwent, R., Cooper, O. R., Tanimoto, H., Volz-
7 Thomas, A., Gilge, S., Scheel, H. E., Steinbacher, M., and Chan, E.: Long-term changes in
8 lower tropospheric baseline ozone concentrations at northern mid-latitudes, Atmos. Chem.
9 Phys., 12, 11485-11504, 10.5194/acp-12-11485-2012, 2012.

10 Rao, A. R., and Hsu, E.-C.: Hilbert-Huang Transform Analysis of Hydrological and
11 Environmental Time Series, 1 ed., Water Science and Technology Library, 60, Springer
12 Netherlands, 2008.

13 Sen, P. K.: Estimates of the regression coefficient based on Kendall's tau, Journal of the
14 American Statistical Association, 63, 1379-1389, 1968.

15 Staehelin, J., Harris, N. R. P., Appenzeller, C., and Eberhard, J.: Ozone trends: A review,
16 Reviews of Geophysics, 39, 231-290, 10.1029/1999RG000059, 2001.

17 Stohl, A., Spichtinger-Rakowsky, N., Bonasoni, P., Feldmann, H., Memmesheimer, M., Scheel,
18 H. E., Trickl, T., Hübener, S., Ringer, W., and Mandl, M.: The influence of stratospheric
19 intrusions on alpine ozone concentrations, Atmospheric Environment, 34, 1323-1354,
20 [http://dx.doi.org/10.1016/S1352-2310\(99\)00320-9](http://dx.doi.org/10.1016/S1352-2310(99)00320-9), 2000.

21 Tang, Q., Prather, M. J., and Hsu, J.: Stratosphere-troposphere exchange ozone flux related to
22 deep convection, Geophys. Res. Lett., 38, L03806, 10.1029/2010gl046039, 2011.

23 Tarasova, O. A., Senik, I. A., Sosonkin, M. G., Cui, J., Staehelin, J., and Prévôt, A. S. H.:
24 Surface ozone at the Caucasian site Kislovodsk High Mountain Station and the Swiss Alpine
25 site Jungfraujoch: data analysis and trends (1990–2006), Atmos. Chem. Phys., 9, 4157-4175,
26 10.5194/acp-9-4157-2009, 2009.

27 Vingarzan, R.: A review of surface ozone background levels and trends, Atmospheric
28 Environment, 38, 3431-3442, <http://dx.doi.org/10.1016/j.atmosenv.2004.03.030>, 2004.

29 Wang, Q. Y., Gao, R. S., Cao, J. J., Schwarz, J. P., Fahey, D. W., Shen, Z. X., Hu, T. F., Wang,
30 P., Xu, X. B., and Huang, R. J.: Observations of high level of ozone at Qinghai Lake basin in
31 the northeastern Qinghai-Tibetan Plateau, western China, Journal of Atmospheric Chemistry,
32 72, 19-26, 10.1007/s10874-015-9301-9, 2015.

33 Wang, T., Ding, A., Gao, J., and Wu, W. S.: Strong ozone production in urban plumes from
34 Beijing, China, Geophys. Res. Lett., 33, L21806, 10.1029/2006gl027689, 2006a.

35 Wang, T., Wong, H. L. A., Tang, J., Ding, A., Wu, W. S., and Zhang, X. C.: On the origin of
36 surface ozone and reactive nitrogen observed at a remote mountain site in the northeastern
37 Qinghai-Tibetan Plateau, western China, Journal of Geophysical Research: Atmospheres, 111,
38 D08303, 10.1029/2005JD006527, 2006b.

39 Wang, T., Wei, X. L., Ding, A. J., Poon, C. N., Lam, K. S., Li, Y. S., Chan, L. Y., and Anson,
40 M.: Increasing surface ozone concentrations in the background atmosphere of Southern China,
41 1994–2007, Atmos. Chem. Phys., 9, 6217-6227, 10.5194/acp-9-6217-2009, 2009.

42 Wang, Y., Konopka, P., Liu, Y., Chen, H., Müller, R., Plöger, F., Riese, M., Cai, Z., and Lü,
43 D.: Tropospheric ozone trend over Beijing from 2002–2010: ozonesonde measurements and
44 modeling analysis, Atmos. Chem. Phys., 12, 8389-8399, 10.5194/acp-12-8389-2012, 2012.

- 1 Xu, X., Lin, W., Wang, T., Yan, P., Tang, J., Meng, Z., and Wang, Y.: Long-term trend of
2 surface ozone at a regional background station in eastern China 1991–2006: enhanced
3 variability, Atmos. Chem. Phys., 8, 2595-2607, 10.5194/acp-8-2595-2008, 2008.
- 4 Xu, X., Tang, J., and Lin, W.: The trend and variability of surface ozone at the global GAW
5 station Mt. WALIGUAN, China, in: "Second Tropospheric Ozone Workshop Tropospheric
6 Ozone Changes: Observations, state of understanding and model performances", WMO/GAW
7 report, WMO, Geneva, 49–55, 2011.
- 8 Xue, L. K., Wang, T., Zhang, J. M., Zhang, X. C., Deliger, Poon, C. N., Ding, A. J., Zhou, X.
9 H., Wu, W. S., Tang, J., Zhang, Q. Z., and Wang, W. X.: Source of surface ozone and reactive
10 nitrogen speciation at Mount Waliguan in western China: New insights from the 2006 summer
11 study, J. Geophys. Res., 116, D07306, 10.1029/2010jd014735, 2011.
- 12 Yang, Y., Liao, H., and Li, J.: Impacts of the East Asian summer monsoon on interannual
13 variations of summertime surface-layer ozone concentrations over China, Atmos. Chem. Phys.,
14 14, 6867-6879, 10.5194/acp-14-6867-2014, 2014.
- 15 Zellweger, C., Hofer, P., and Buchmann, B.: System and Performance Audit of Surface Ozone
16 and Carbon Monoxide at the China GAW Baseline Observatory Waliguan Mountain, WCC-
17 Empa Report 00/3Rep., 46 pp, Empa, Dübendorf, Switzerland,
18 http://gaw.empa.ch/audits/WLG_2000.pdf, 2000.
- 19 Zellweger, C., Klausen, J., and Buchmann, B.: System and Performance Audit of Surface
20 Ozone Carbon Monoxide and Methane at the Global GAW Station Mt. Waliguan, China,
21 October 2004, WCC-Empa Report 04/3Rep., 52 pp, Empa, Dübendorf, Switzerland,
22 http://gaw.empa.ch/audits/WLG_2004.pdf, 2004.
- 23 Zellweger, C., Klausen, J., Buchmann, B., and Scheel, H.-E.: System and Performance Audit
24 of Surface Ozone, Carbon Monoxide, Methane and Nitrous Oxide at the GAW Global Station
25 Mt. Waliguan and the Chinese Academy of Meteorological Sciences (CAMS) China, June 2009,
26 WCC-Empa Report 09/2Rep., 61 pp, Empa, Dübendorf, Switzerland,
27 https://www.wmo.int/pages/prog/arep/gaw/documents/WLG_2009.pdf
- 28

1 [, 2009.](#)

2 [Zhang, F., Zhou, L. X., Novelli, P. C., Worthy, D. E. J., Zellweger, C., Klausen, J., Ernst, M.,](#)
3 [Steinbacher, M., Cai, Y. X., Xu, L., Fang, S. X., and Yao, B.: Evaluation of in situ](#)
4 [measurements of atmospheric carbon monoxide at Mount Waliguan, China, Atmos. Chem.](#)
5 [Phys., 11, 5195-5206, 10.5194/acp-11-5195-2011, 2011.](#)

6 [Zheng, X. D., Shen, C. D., Wan, G. J., Liu, K. X., Tang, J., and Xu, X. B.: \$\sim\(10\)\text{Be}/\sim 7\text{Be}\$](#)
7 [implies the contribution of stratosphere-troposphere transport to the winter-spring surface \$\text{O}_3\$](#)
8 [variation observed on the Tibetan Plateau, Chin. Sci. Bull., 56, 84-88, 2011.](#)

9 [Zhu, B., Akimoto, H., Wang, Z., Sudo, K., Tang, J., and Uno, I.: Why does surface ozone peak](#)
10 [in summertime at Waliguan?, Geophysical Research Letters, 31, L17104,](#)
11 [10.1029/2004GL020609, 2004.](#)

12

13

1 Table 1 The linear slope, 95% confidence interval (in ppbv 10a⁻¹) and the p-values (in
 2 parenthesis) of all-year and seasonal average surface ozone mixing ratio for the all-day data and
 3 for the daytime and nighttime data subsets during 1994 to 2013

Data subset	All year	MAM	JJA	SON	DJF
All Day	2.5±1.7 (<0.01)	2.4±1.1 (<0.01)	1.5±1.9 (0.12)	2.8±1.1 (<0.01)	1.4±0.9 (<0.01)
Day	2.4±1.6 (<0.01)	2.4±1.1 (<0.01)	0.7±1.8 (0.41)	2.7±1.0 (<0.01)	1.5±0.9 (<0.01)
Night	2.8±1.7 (<0.01)	2.4±1.2 (<0.01)	2.2±2.0 (0.04)	2.9±1.1 (<0.01)	1.3±1.0 (0.01)

4
5

1

2 Table 2 The linear ~~slopes~~slopes (in ppbv $10a^{-1}$) and the 95% confidence ~~interval~~intervals of all-
 3 year and seasonal average surface ozone mixing ratio ~~during 1994 to 2013 at~~at WLG and other
 4 north hemispheric high altitude GAW sites.

Station (Location)	Time Span	All Year	MAM	JJA	SON	DJF	Reference
Mauna Loa, USA (19.5N, 155.6W, 3397 m asl)	1991-2010	3.1±0.7					(Oltmans et al., 2013)
Izaña, Spain (28.3N, 16.5W, 2367 m asl)	1991-2010	1.4±0.5					(Oltmans et al., 2013)
Waliguan, China (36.3N, 100.9E, 3816 m asl)	1994-2013	2.5±1.7	2.4±1.1	1.5±1.9	2.8±1.1	1.4 ±0.9	This work
Rocky, USA (40.3N, 105.6W, 2743 m asl)	1991-2010	3.3±0.5					(Oltmans et al., 2013)
Pinadale, USA (42.9N, 109.8W, 2743 m asl)	1991-2010	-0.5±0.4					(Oltmans et al., 2013)
Kislovodsk, Russia (43.70N, 42.70E, 2070 m asl)	1991-2006	-3.7±1.4	-2.0±2.0	-1.4±2.4	-6.0±2.1	-3.0±2.5	(Tarasova et al., 2009)
Whiteface, USA (44.4N, 73.9W, 1484 m asl)	1991-2010	-2.2±0.6					(Oltmans et al., 2013)
Jungfraujoch, Switzerland (46.5N, 8.0E, 3580 m asl)	1990-2008	3.2±1.8	3.3±2.2	2.2±2.8	3.3±1.6	4.9±1.7	(Cui et al., 2011)
Zugspitze, Germany (47.4N, 11.0E, 2960 m asl)	1991-2010	0.5±0.4					(Oltmans et al., 2013)

5

6

1

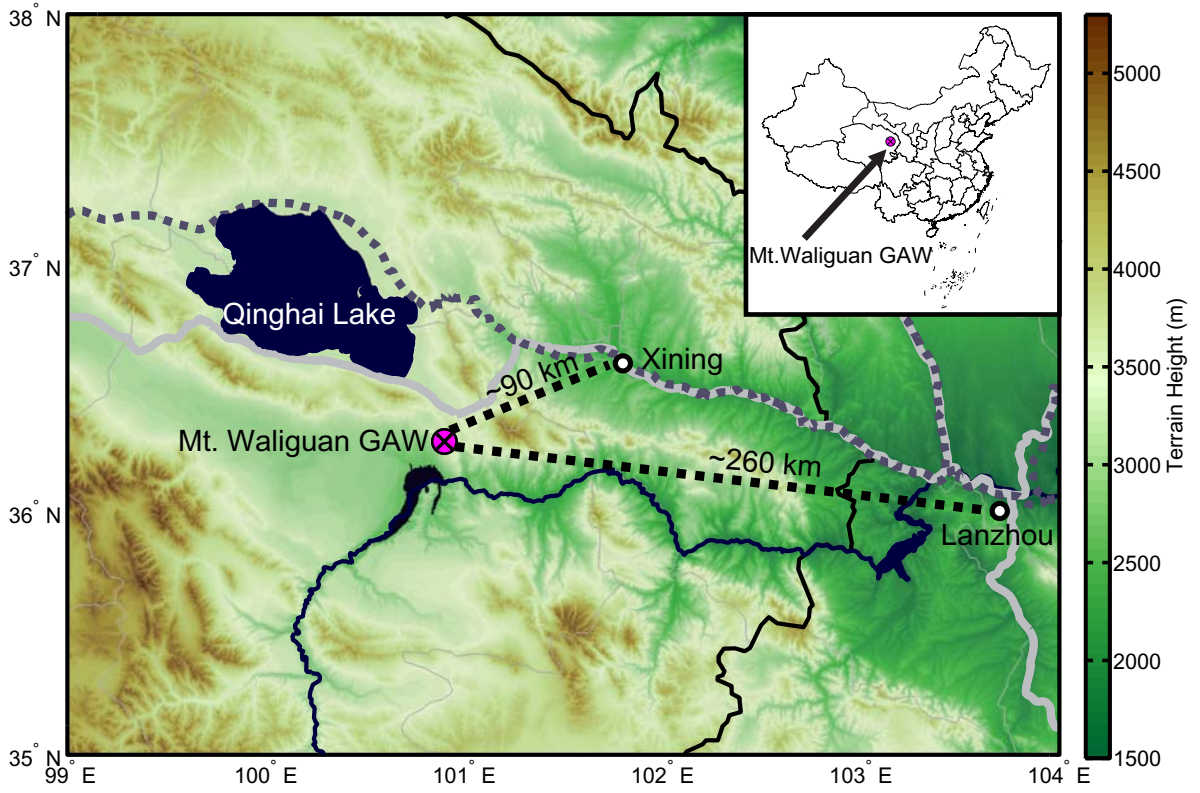
2 Table 3 Modified Mann-Kendall trend test on segments based on the last IMF.

Segment	Time Range	Slope of c5	Modified Mann-Kendall test (z)	Slope of O ₃ (ppbv 10a ⁻¹)
1	Aug. 1994- Jun. 1997	-	No significant trend (z =1.42)	2.7
2	Jul. 1997-May 2002	+	Significant upward trend (z =3.66)	4.2
3	Jun. 2002-Apr. 2008	-	Significant upward trend (z =3.57)	3.0
4	May 2008-Jul. 2013	+	Significant upward trend (z = 3.42)	3.6

3

4

1

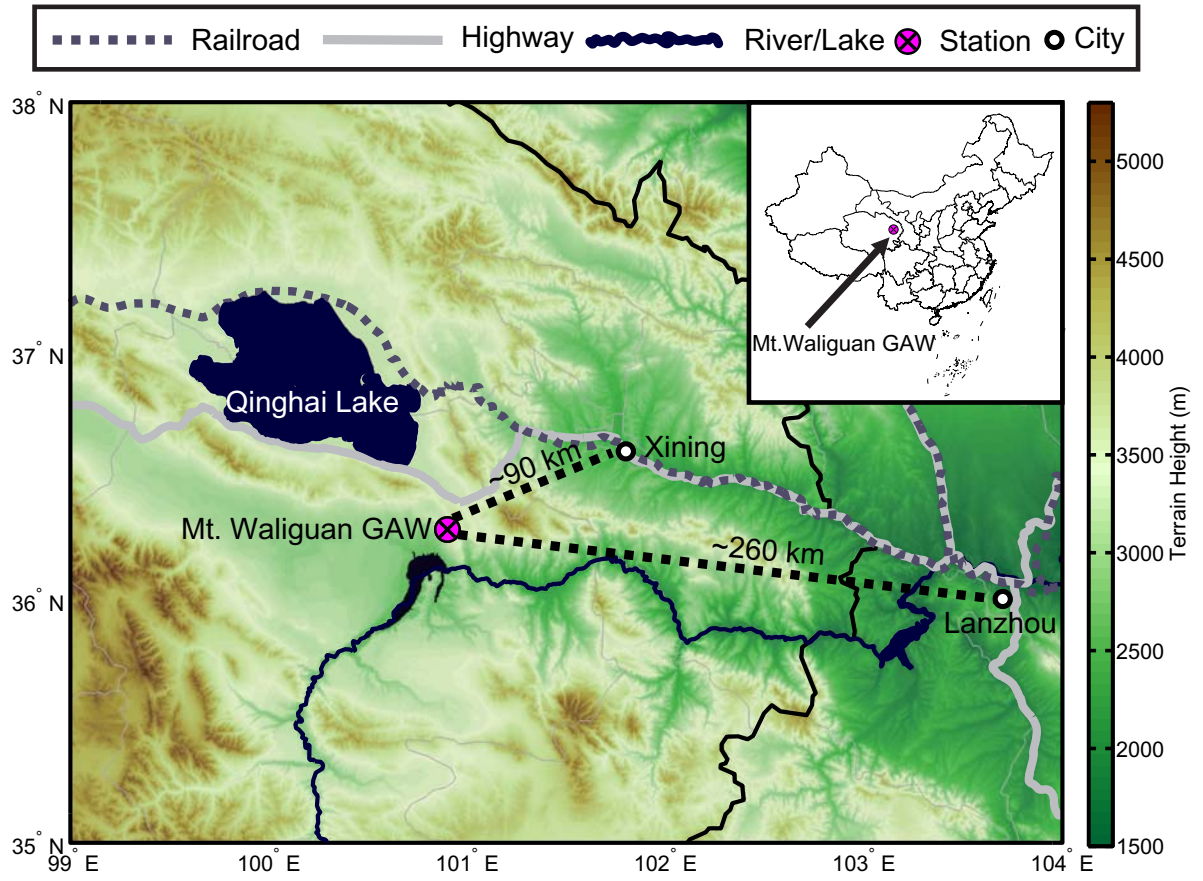


2

3

4

1

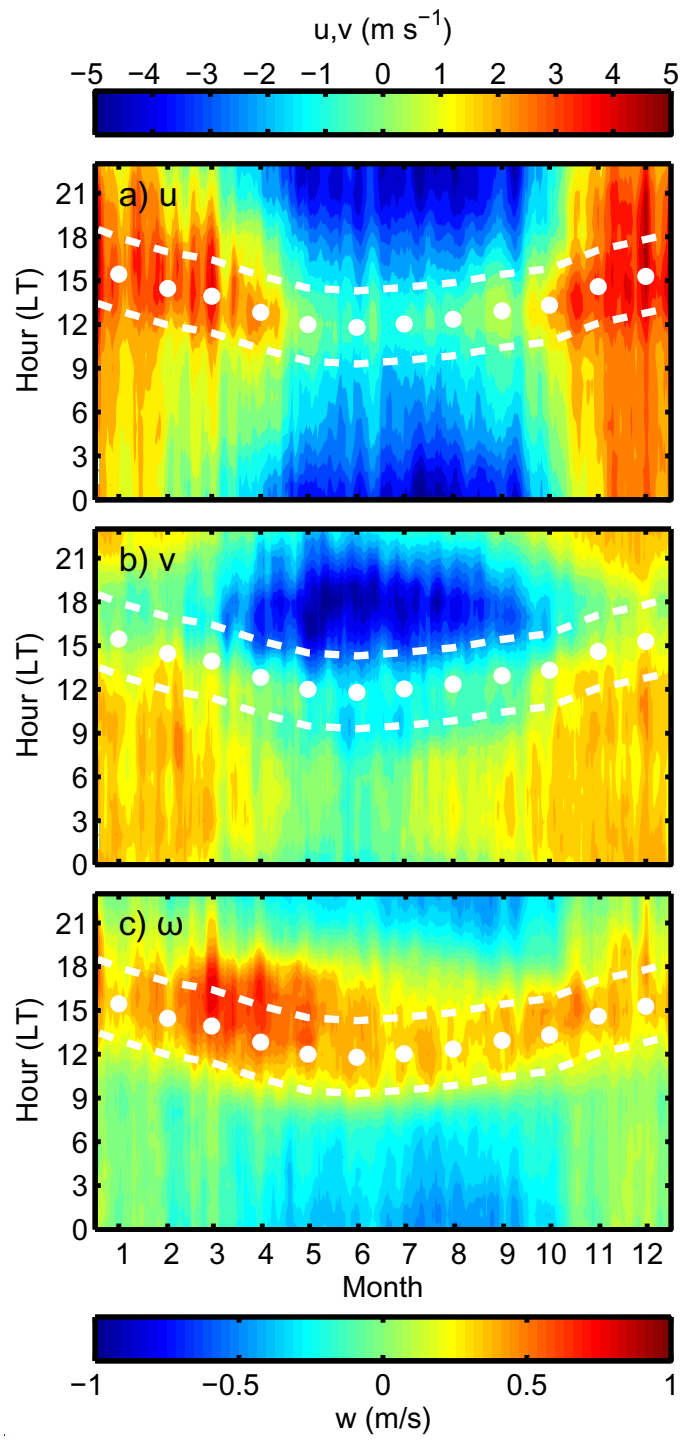


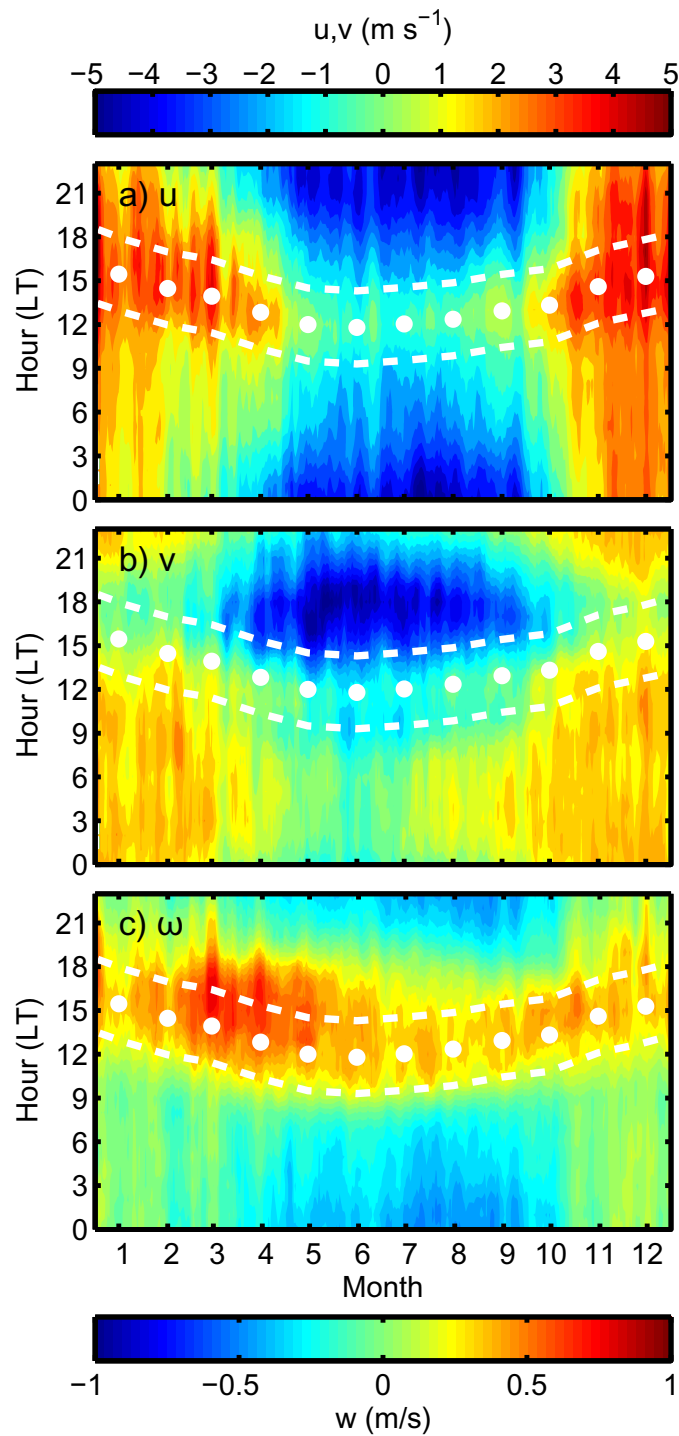
2

3 Figure 1 The location of the Mt. Waliguan GAW site and the two major cities in its vicinity.

4 The shading stands for the topographic height.

5

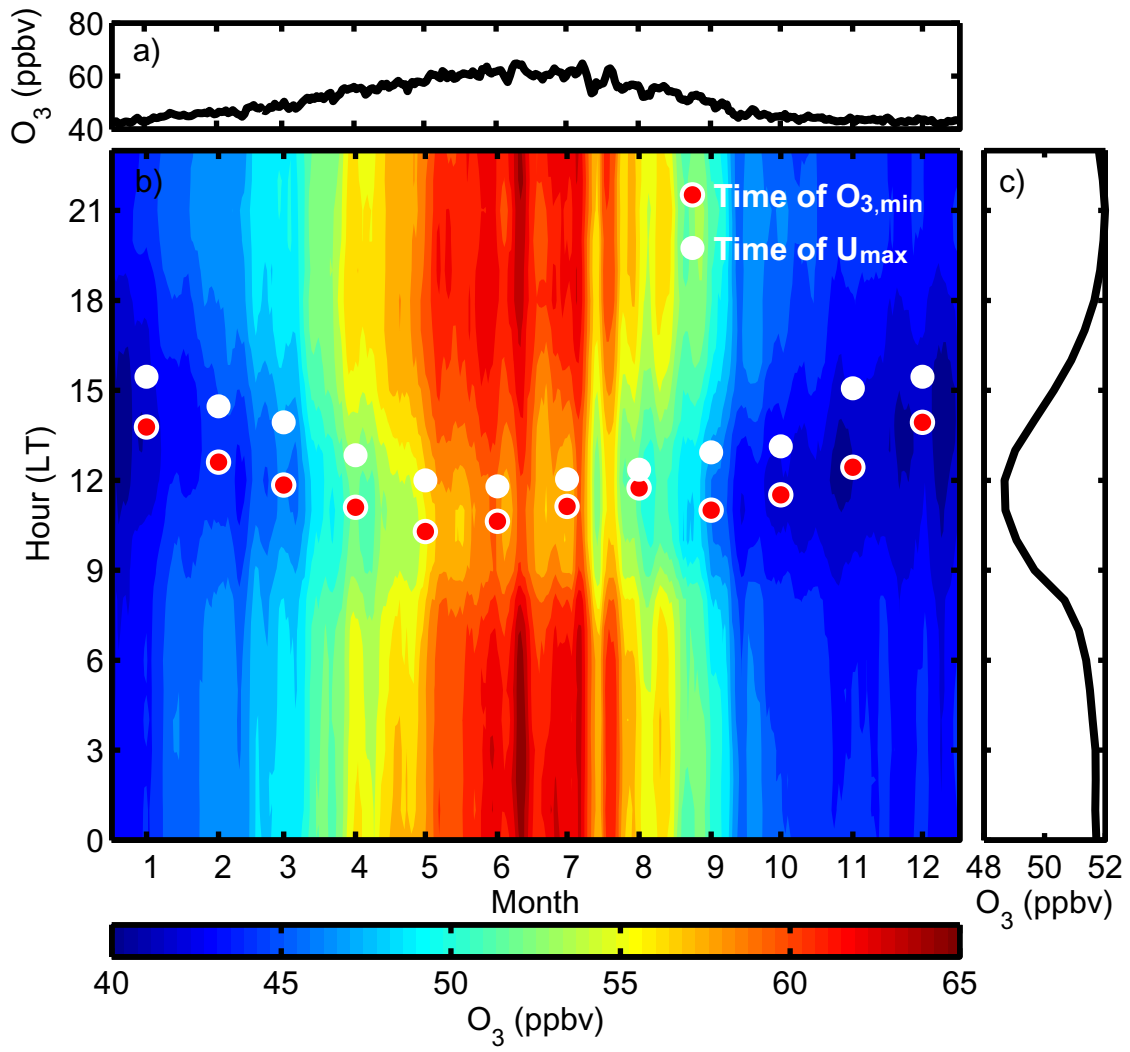




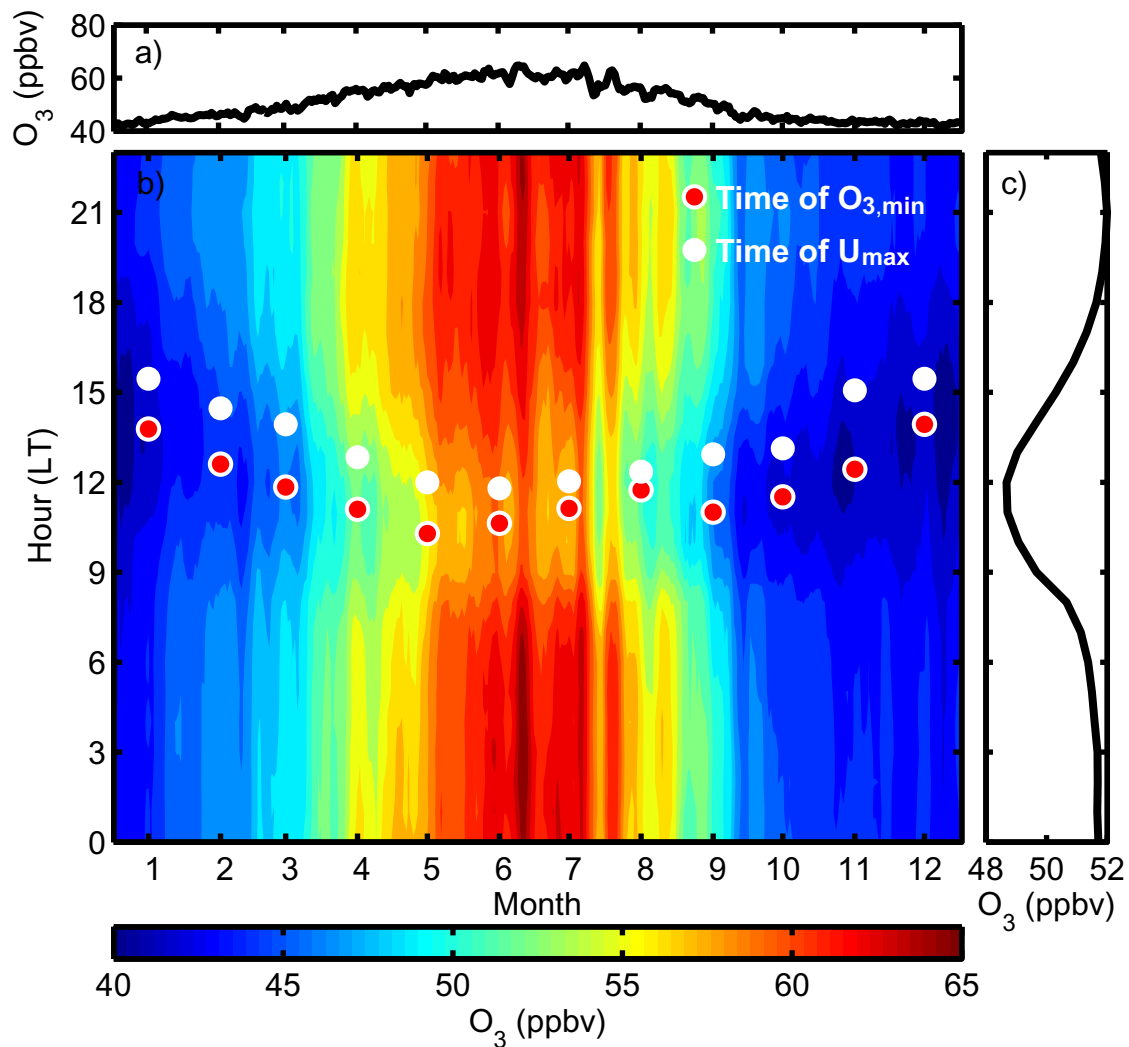
1

2 Figure 2 The average season-diurnal variation of surface zonal (a), meridional (b) and vertical
 3 (c) wind velocity on top of Mt. Waliguan during 1995-2013. The monthly average hour
 4 associated with the diurnal maximum zonal wind speed is given by the white dots, the daytime
 5 range is provided by the white dashed lines, which covers 6 hours centered around the white
 6 dots.

7



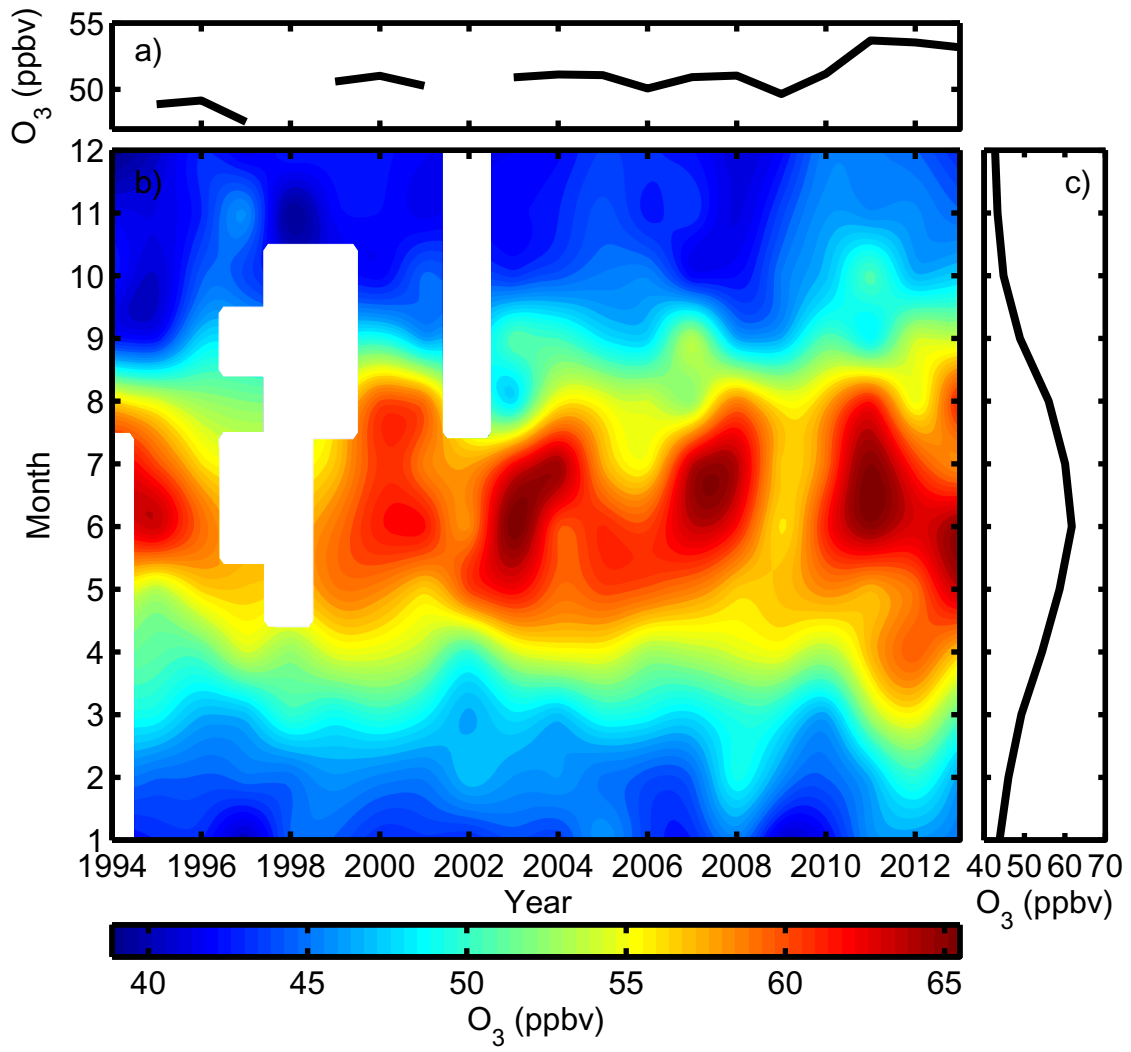
1



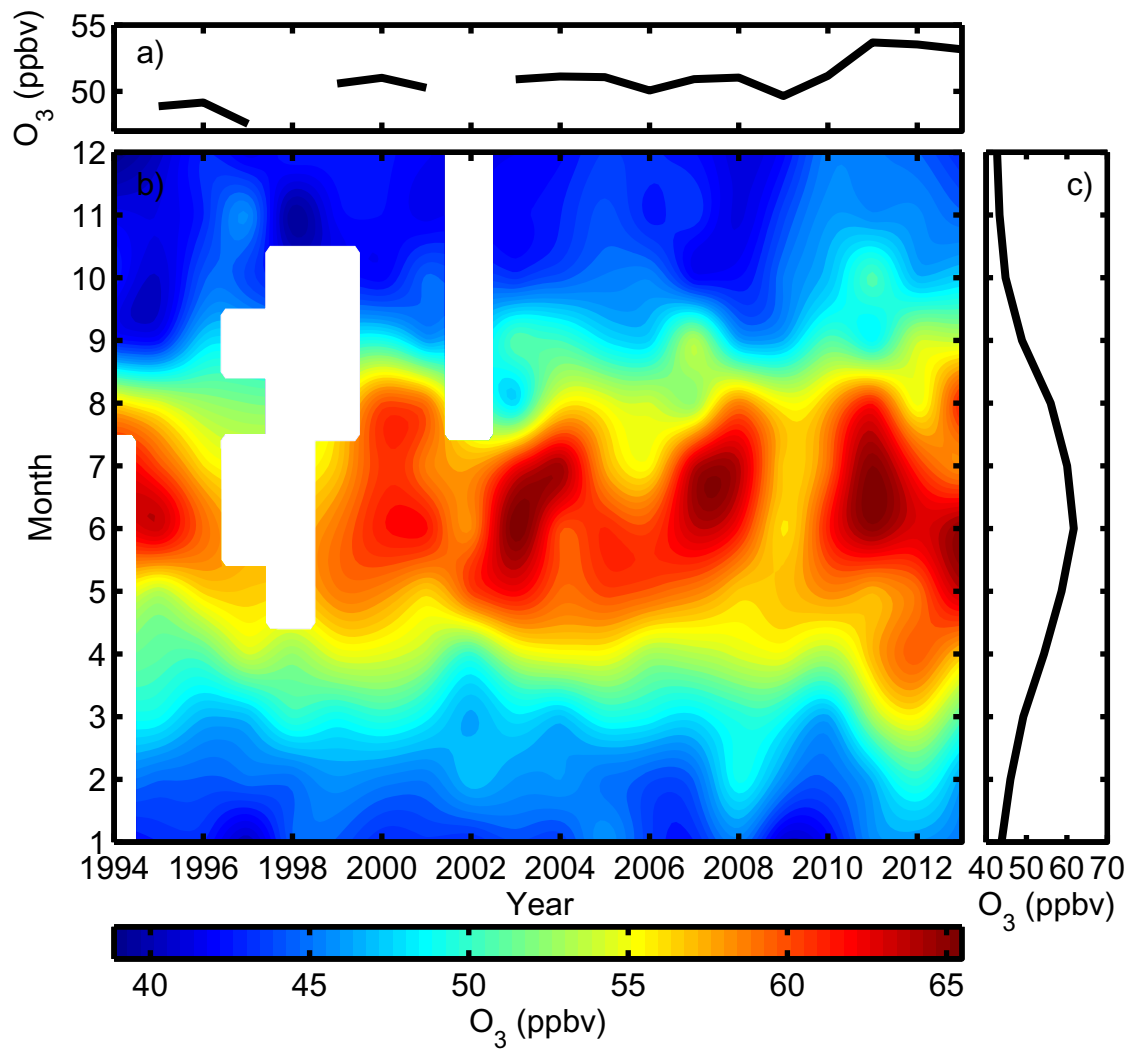
1

2 Figure 3 The average seasonal variation (a), season-diurnal variation (b) and diurnal variation
 3 (c) of ozone during 1995 to 2013. ~~White~~The red and white dots ~~stands for~~indicate the monthly
 4 average local ~~times~~ associated with the diurnal minimum ozone, ~~and~~ the ~~white dashed line~~
 5 ~~stands for a 6 hours range centered around the white dots~~diurnal maximum zonal wind (U_{max}),
 6 ~~respectively~~.

7



1



1

2 Figure 4 The average inter-annual variation (a), season-annual variation (b) and seasonal
 3 variation (c) of ozone during 1994 to 2013.

4

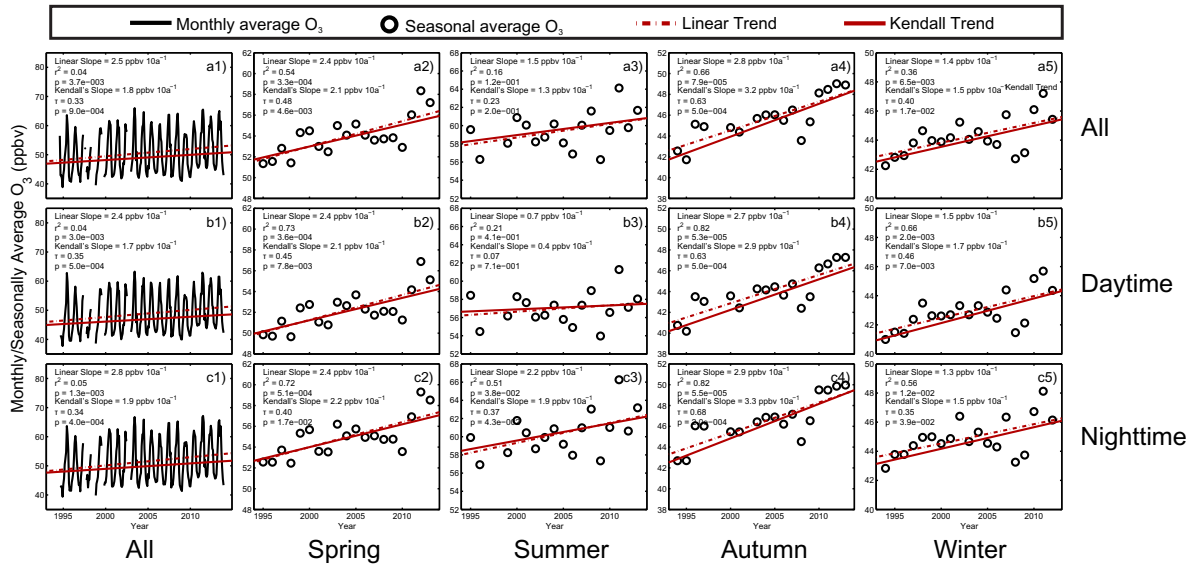
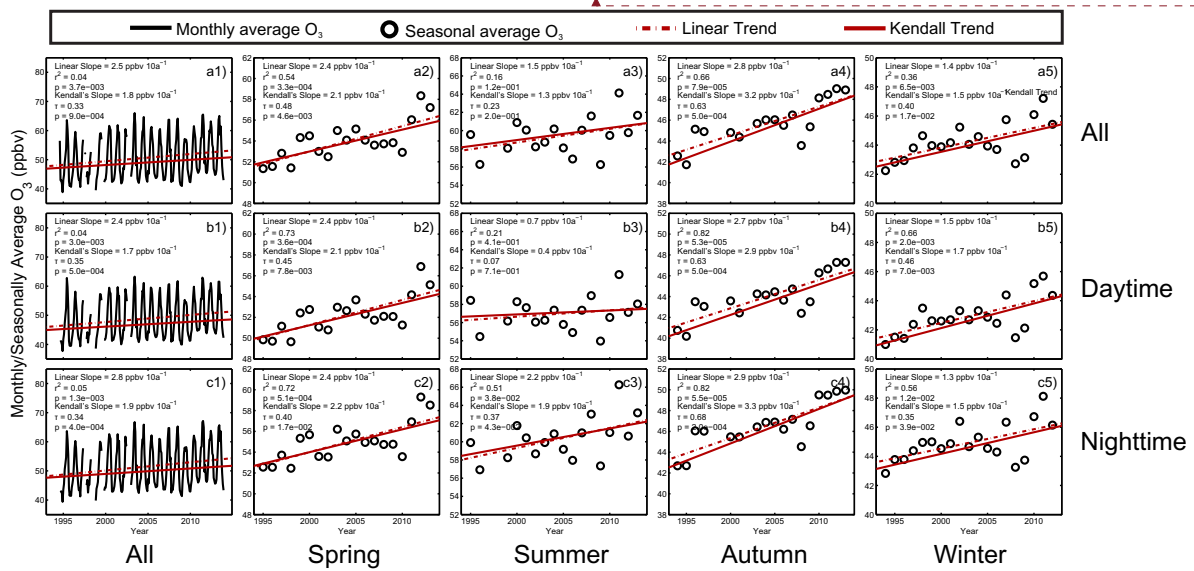
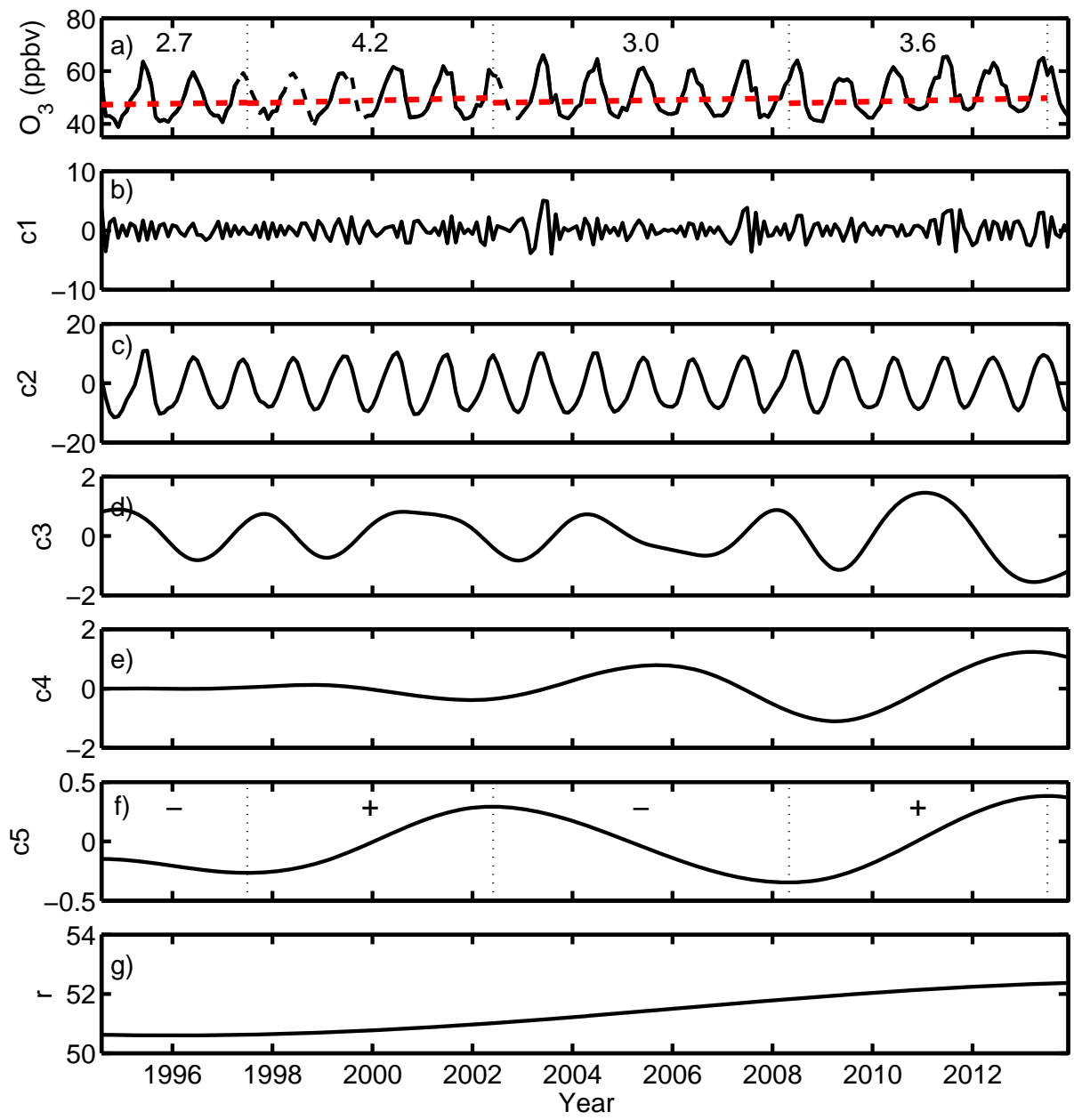
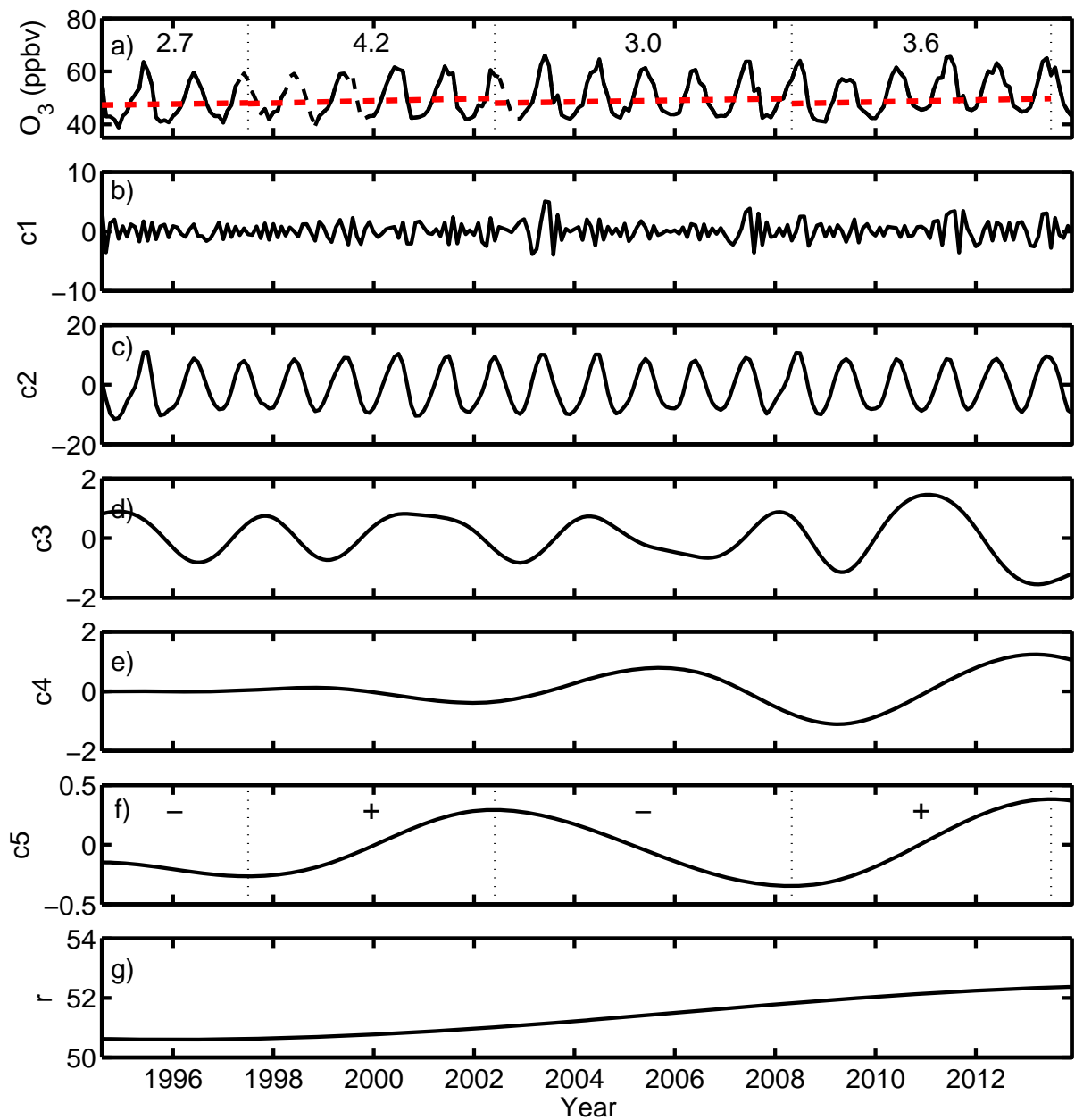


Figure 5 1) Monthly, 2) spring (MAM), 3) summer (JJA), 4) autumn (SON) and 5) winter time average all day (a), daytime (b) and nighttime (c) surface ozone mixing ratio during 1994 to 2013 (black solid line curves or black circles) and its variation trend (red lines: dotted line stands for the linear variation and solid line stands for the Kendall's variation slope).

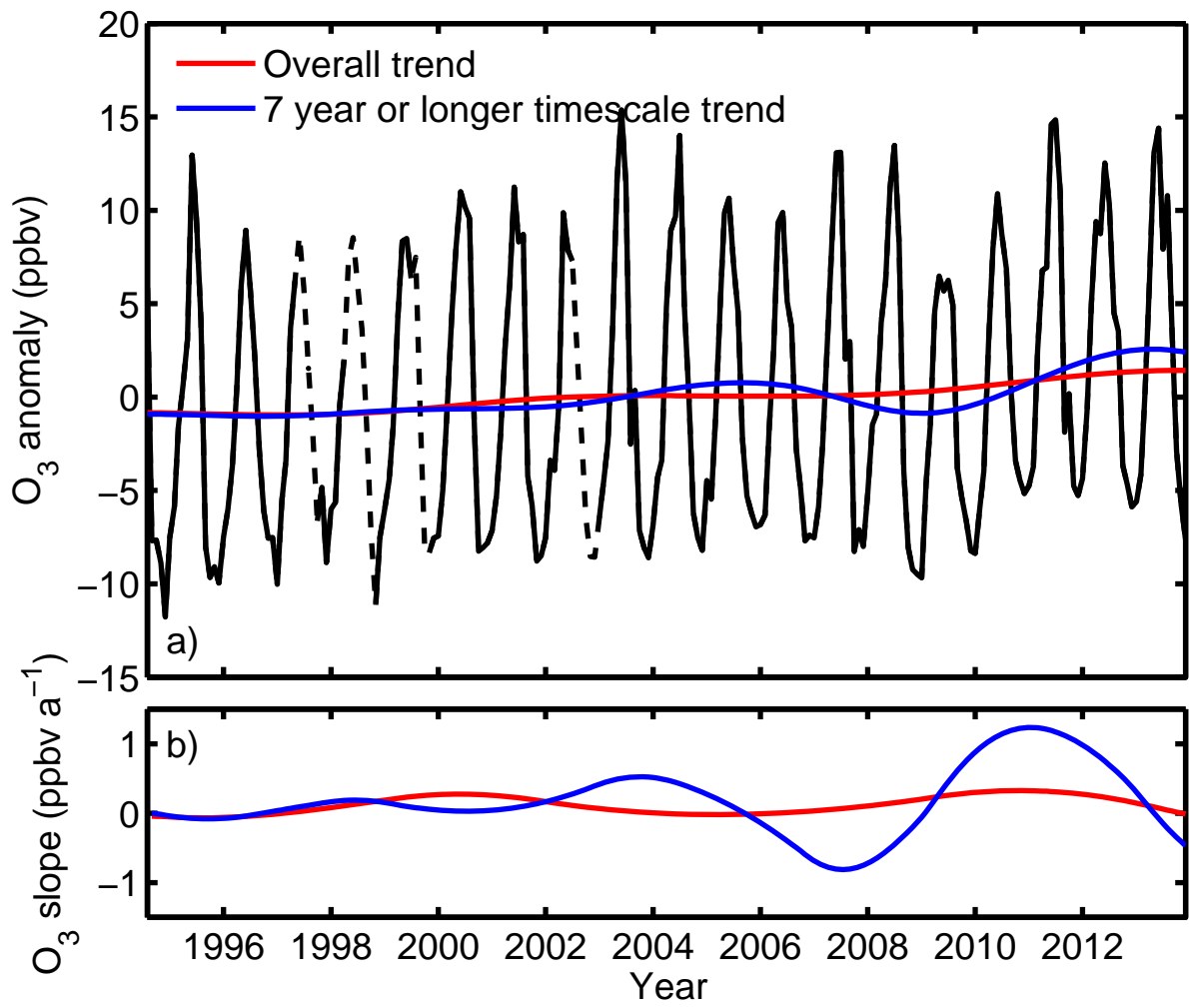


1

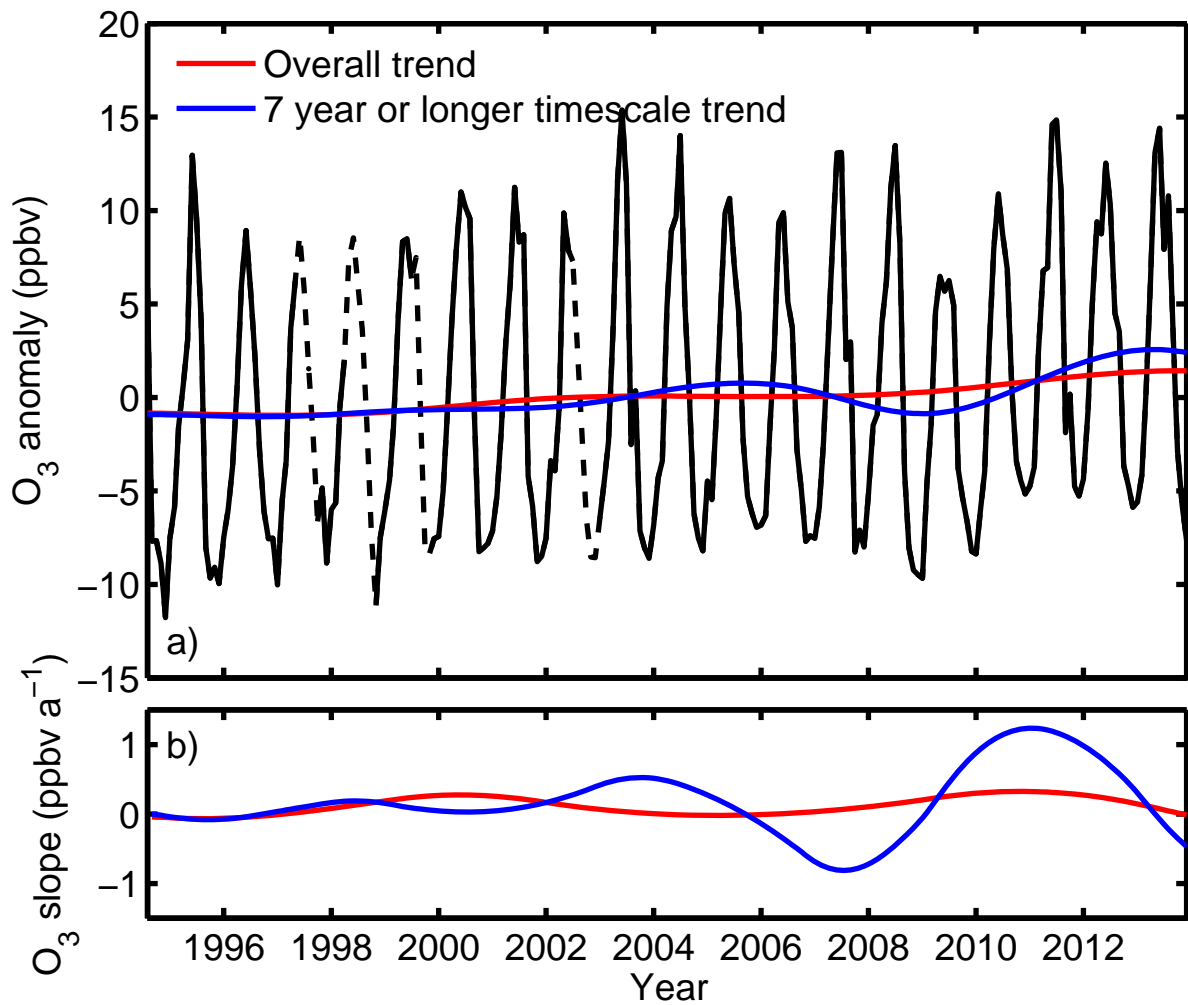


1
 2 Figure 6 The interpolated monthly average ozone mixing ratio at WLG from 1994 to 2013 (the
 3 interpolated data given in dashed lines, a) and its intrinsic mode functions c1-c5 (b-f, from the
 4 lowest ~~order IMF~~ to the highest order IMF) and its residue, r (g). The time segments in (a) were
 5 determined by the slope of the c5. The red slashed lines are the Kendall's trends and the
 6 numbers are the Kendall's ~~slopes~~ (in ppbv $10a^{-1}$).

7

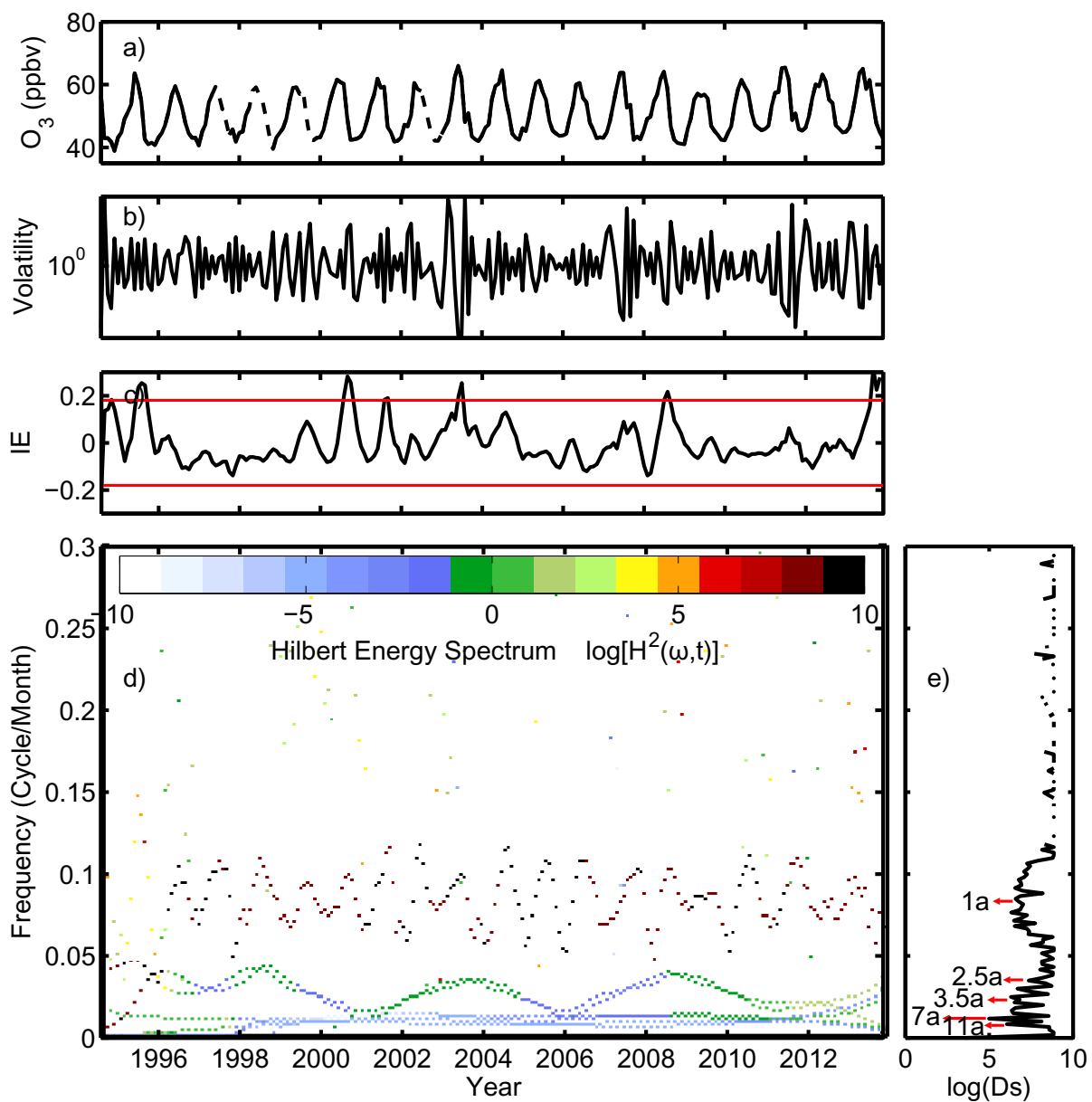


1

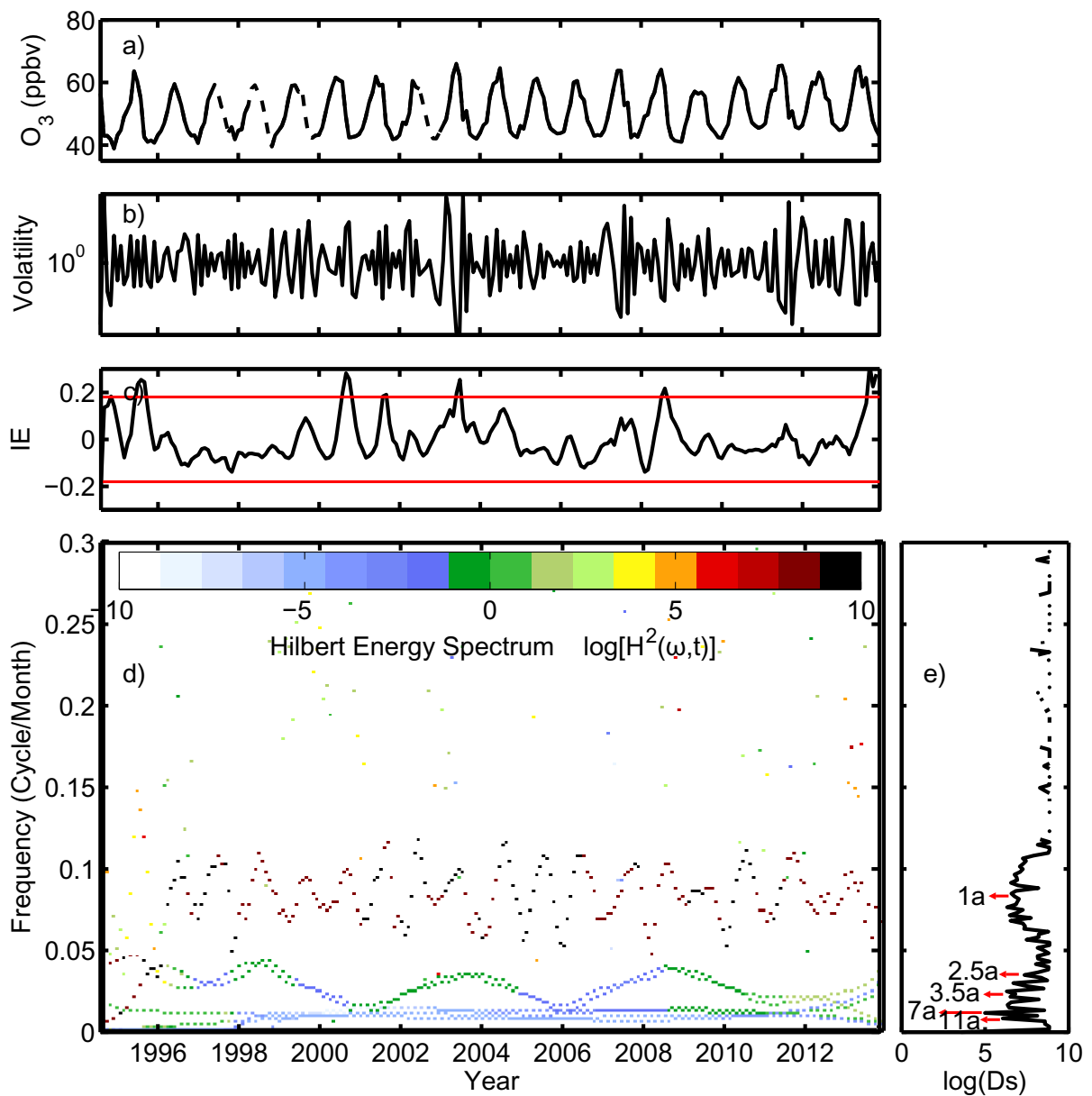


1
 2 Figure 7 a) The anomaly of the interpolated monthly average ozone (black line), with the dashed
 3 line segments representing values interpolated using the method in section 2.5), the sum of last
 4 IMF and the residual (c5+r, red line), and the sum of the last two IMFs and the residual
 5 (c4+c5+r, blue line); b) the slope of the sum of last IMF and the residual (c5+r, red line) and
 6 the sum of the last two IMFs and the residual (c4+c5+r, blue line).

7



1



1
 2 Figure 8 The interpolated monthly average ozone mixing ratio signal at Mt. WLG during 1994
 3 to 2013 (a), the volatility (b), the normalized mean value of the instantaneous energy (red lines:
 4 $\pm 2\sigma$) (c), Hilbert Energy Spectrum (d) and the degree of stationarity (e).

5
 6
 7